Support Vector Machines (SVMs) Based Framework for Classification of Fallers and Non-fallers

Jian Zhang

Dissertation submitted to the faculty of the Virginia Polytechnic Institute and State University in partial fulfillment of the requirements for the degree of

Doctor of Philosophy

In

Industrial and Systems Engineering

Thurmon E. Lockhart, Chair

Michael J. Agnew, Co-Chair

Dong S. Ha

Karen A. Roberto

Robert H. Sturges

May 5, 2014

Blacksburg, VA

Keywords: Support vector machines, Machine learning, Fallers and non-fallers, Gait and postural parameters, Feature extraction, Robustness

Support Vector Machines (SVMs) Based Framework for Classification of Fallers and Non-fallers

Jian Zhang

ABSTRACT

The elderly population is growing at a rapid pace, and falls are a significant problem facing adults aged 65 and older in terms of both human suffering and economic losses. Falls are the leading cause of mortality among older adults, and non-fatal falls result in reduced function and poor quality of life for older adults. Although much is known about the mechanisms and contributing risk factors relevant to falls, falls still remain a significant problem associated with this age group. Therefore, new strategies and knowledge need to be introduced to understand and prevent falls.

Studies show that early detection of impaired mobility is critical to the prevention of falls. In this study, the relationship between gait and postural parameters and falls among elderly participants using wearable inertial sensors was investigated. As such, the aim of this study is to investigate the critical gait and postural parameters contributing to falls, then further to classify fallers and non-fallers by utilizing gait and postural parameters and machine learning techniques, e.g. support vector machines (SVMs). Additionally, as the assessment of fall risk is linked to noisy environment, it is important to understand the capability of the SVM classifier to effectively address noisy data. Therefore, the robustness of the SVM classifier was also investigated in this study.

In summary, the presented work addresses several challenges through research on

the following three issues: 1) the significant differences in gait and pastoral parameters between fallers and non-fallers; 2) a machine learning based framework for classification of fallers and non-fallers by using only one IMU located at the sternum; and 3) robustness of SVM classifier to classify fallers and non-fallers in a noisy environment.

The machine learning based framework developed in this dissertation contribute to advancing the state-of-art in fall risk assessment by 1) classifying fallers and non-fallers from a single IMU located at the sternum; 2) developing machine learning method for classification of fallers and non-fallers; and 3) investigating the robustness of SVM classifier in a noisy environment.

This dissertation is dedicated to my Mother and Father for their endless love, support, and encouragement.

ACKNOWLEDGEMENT

This dissertation would not have been possible without the support of many people, therefore it is my great pleasure to thank them for their kind help, support, and contributions.

First I would like to convey my sincere respect and many thanks to my primary advisor, Dr. Thurmon E. Lockhart, for his continuous support, encouragement and advice throughout my Ph.D. study. It has been a pleasure working with him during the past few years. He is truly my mentor and friend.

I would also like to thank my co-advisor, Dr. Michael J. Agnew, and other committee members, Dr. Dong S. Ha, Dr. Karen A. Roberto, and Dr. Robert H. Sturges, for their insightful comments and suggestions, which helped me make this work stronger.

I would also like to thank all my collaborators and labmates, Rahul Soangra, Christopher Frames, Charlie Chuleui Chung, Peter Fino, and Manutchanok Jongprasithporn, for their friendship, support, assistant, and discussions.

My special thanks go to my friends in Virginia Tech, for making my everyday life colorful. Without them I could not have made it through these years.

Finally, I send my largest thank you to my mother Wang Guofen and my father Zhang Shihua. Although you have not been here physically throughout my years in U.S., I always feel your support and love.

Contents

List of Figures

List of Tables

Chapter 1 INTRODUCTION

1.1 Motivation

The elderly population is growing at a rapid pace, and is expected to increase further in the coming years [1]. In the U.S., the number of persons aged 65 and older is projected to more than double, from 38.7 million to 88.5 million between 2008 and 2050 [2] (Figure 1-1).

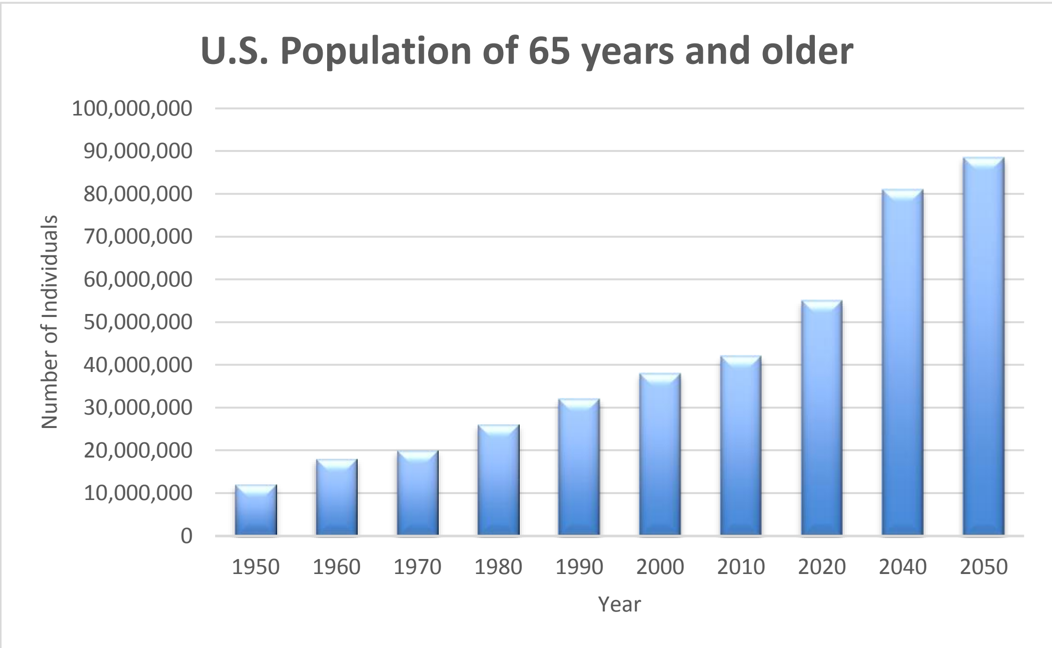

Figure 1-1: Population of 65 years and older in the U.S. from 1950 to 2050 (U.S. Bureau of the Census).

Fall accidents are a significant problem facing older adults in terms of both human physical suffering and economic losses. Falls are the leading cause of mortality among older adults, with non-fatal falls also resulting in reduced functional abilities and poor quality of life [3]. Approximately, 35-40% of healthy, community dwelling older adults fall annually; after the age of 75, the rates are higher [4]. From 2001 to 2010, fall-related fatalities have increased by about 1.7 fold, from 15,764 to 26,852. For persons aged 65 years and older, the number increased from 11,746 to 21,759 [5] (Figure 1-2 (a)). In addition, the non-fatal injuries have increased from 7,860,598 to 8,991,813 from the year 2001 to 2012. In 2012, almost 9.0 million non-fatal injuries were experienced by persons of all ages, with 2.4 million non-fatal injuries suffered by persons aged 65 and over (Figure 1-2 (b)) [6]. Thus, more than 25% of the older adult population experienced non-fatal fall-related injuries. Non-fatal injuries in the older age group are consistently among the top causes of injuries across all age groups, with falls being the leading cause of non-fatal injuries that necessitated treatment in hospital emergency departments. In 2010, there were 2.3 million non-fatal injuries among older adults treated in emergency departments, with over 662,000 of these patients requiring hospitalization [7].

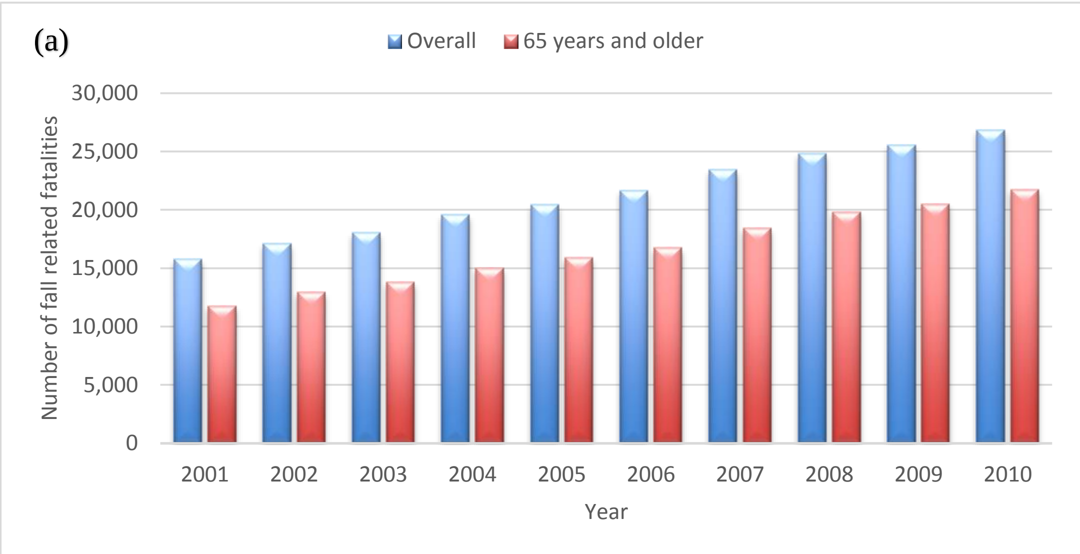

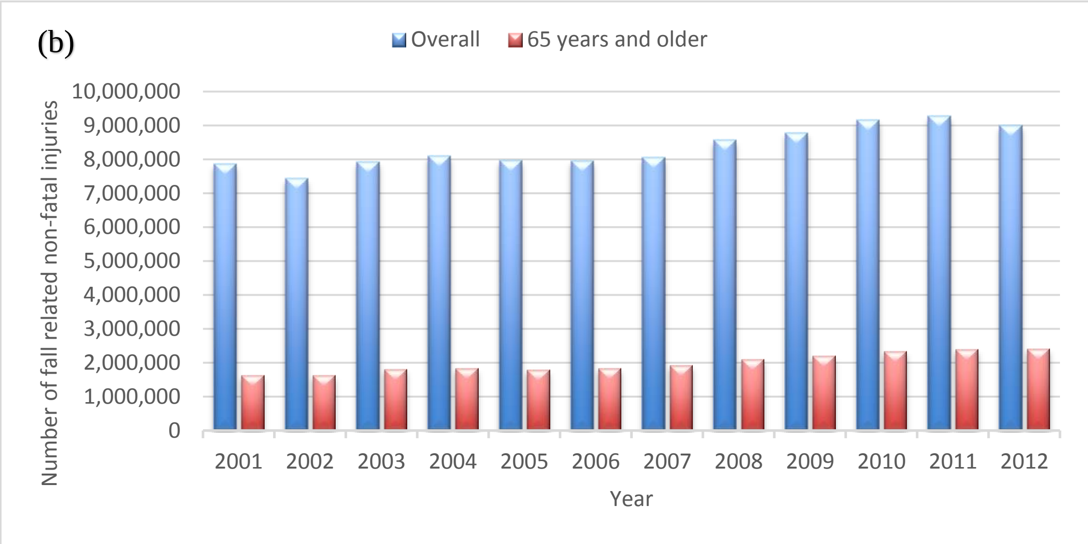

Figure 1-2: (a) Fall related fatalities in the U.S. from 2001 to 2010, and (b) non-fatal injuries in the U.S. from 2001 to 2012.

While falls primarily contribute to physical suffering and functional impairments, they are also responsible for increasing medical costs, absenteeism, and negative psychological and social consequences, such as fear of falling and post-fall anxiety syndrome. Furthermore, the loss of confidence to ambulate safely leads to psychological limitations and dependence. Moreover, the total cost of fall related injuries for the persons aged 65 and older was \$19.2 billion in 2000 [8], \$30 billion in 2010, and is expected to increase to \$54.9 billion by 2020 [9] (Figure 1-3). Fall-related injuries account for 6% of all medical expenditures for older persons in the U.S. [10]. Approximately 95% of all hip fractures in the U.S. are the results of falling; as such, hip fractures among older adults rank as one of the most serious public health problems in the U.S., with costs expected to exceed \$43.8 billion by the year 2020 [11].

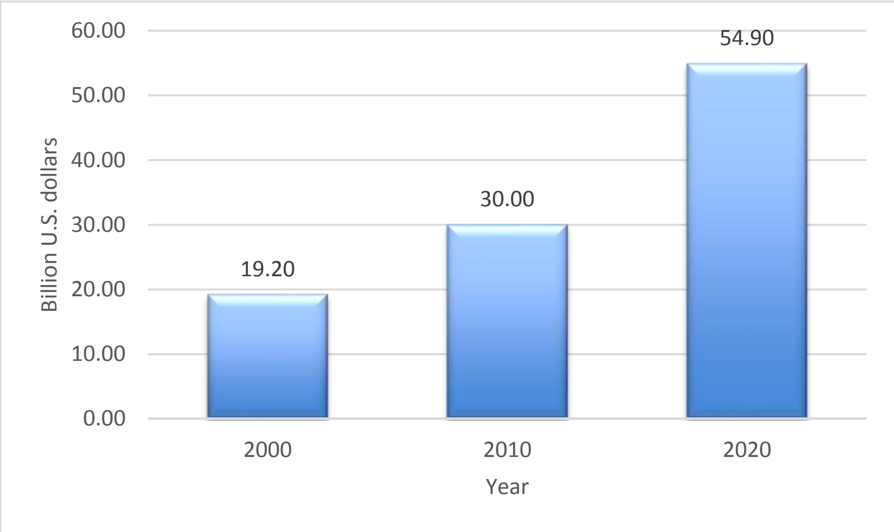

Figure 1-3: Cost of fall injuries for people 65 and older in 2000, 2010, and 2020.

To reduce the personal and economic losses associated with falls, a considerable amount of research has been conducted to investigate the risk factors of fall accidents, and how they contribute to high occurrence of injuries and fatalities. Studies classify fall risk factors into two categories: intrinsic (e.g. muscle weakness, poor balance, functional and cognitive impairment, visual deficits, etc.) [12-16] and extrinsic (e.g. adverse drug interactions, use of prostheses, use of constraints, poor lighting, loose carpets, lack of bathroom safety) [17, 18]. Most falls are precipitated by both extrinsic factors, which are induced by environmental hazards and are influenced by situational context, and intrinsic factors, which are the result of medical illness.

Although much has been reported regarding the mechanism and contributing risk factors to fall accidents, fall accidents still remain a significant problem for older adults. Numerous studies have proposed various types of intervention solutions [14, 19-21]; however, most of the intervention approaches fail to reduce fall risks and prevent significant injuries. This is due to the time between onset of a fall event and the administration of fall intervention techniques [22]. Therefore, identification of fall-prone individuals is a significant and critical research area, since it can provide timely interventions prior to a fall occurrence.

1.2 Research Objective

The primary goal of this research is to identify differences in gait and postural parameters between fallers and non-fallers; and further, to classify fallers and non-fallers using machine learning techniques. Pursuant to this goal, the specific aims of this research are to:

1. Analyze gait and postural characteristics for mobility analysis and fall risk assessment. The acquisition and analysis of gait and postural characteristics can provide an effective tool for evaluating and quantifying gait problems associated with fall-prone individuals. Therefore, we investigated the relationship between gait and postural parameters and fall risks.

Hypothesis 1-a: There are significant differences in gait parameters, such as walking speed, step length, step width, etc., between fallers and non-fallers.

Hypothesis 1-b: There are significant differences in postural parameters, involved in sit-to-stand, sit-to-walk transition or postural stability, between fallers and non-fallers.

2. Investigate a support vector machine (SVM) classifier to distinguish fallers and non-fallers. The SVM classifier was developed to recognize fallers and non-fallers, by extracting crucial features from gait patterns.

Hypothesis 2-a: An SVM classifier has the potential to classify fallers and non-fallers.

Hypothesis 2-b: One sensor located on the trunk is satisfactory to identify fallers and non-fallers.

3. Evaluate the performance of the SVM classifier in a noisy environment. Specifically, investigate the effect of two parameters involved in an SVM algorithm on the classification accuracy.

Hypothesis 3-a: The parameters in the SVM algorithm are able to adjust themselves according to different noisy environments, in order to achieve good classification accuracy.

Hypothesis 3-b: The SVM classifier is robust enough to classify fallers and non-fallers in noisy environments.

1.3 Organization

There are six chapters in this dissertation. The first chapter introduces the motivation for the research presented in this dissertation. Specific aims and hypotheses are expanded upon to classify the research objective of this dissertation. Chapter 2 provides a compendium of literature related to human physical activity assessment and fall risk assessment. The first section briefly presents research findings concerning risk factors for falls among older adults; subsequently, the second section introduces various classifiers and their applications in human physical activity classification. Specifically, the theoretical aspects of support vector machines (SVMs) are illustrated, and then the advantages and disadvantages of SVMs are discussed. Finally, various fall risk assessment approaches are investigated. Specifically, inertial measurement units (IMUs) relevant to fall risk assessment methods are emphasized, since IMUs were used for data collection in our study.

Chapter 3 presents study I, the investigation of the effect of gait and postural parameters on fall risk. This chapter starts with study objective, and then corresponding experiments are designed to validate the hypotheses in this study. Afterwards, gait and postural parameters are analyzed between fallers and non-fallers. The relationship of gait and postural parameters between fallers and non-fallers is identified and compared with previous studies.

Chapter 4 demonstrates study II, an explicit description for the methods to identify fallers and non-fallers using only one IMU located at the sternum. The results are analyzed to confirm the potential of the SVM classifier to classify fallers and non-fallers using only one IMU wearable sensor.

Chapter 5 presents study III, the performance of the SVM algorithm and the effects of two parameters involved in the SVM algorithm, i.e. the soft margin constant C and the kernel function parameter γ are investigated. The changes associated with adding white noise on the classification accuracies are further discussed.

The sixth and final chapter, Chapter 6, concludes the dissertation with a summary of the contributions of the dissertation, limitations of the studies, and some recommendations for extending the current research for future investigations.

Chapter 2 BACKGROUND AND LITERATURE REVIEW

This chapter begins with a discussion of the key research findings concerning risk factors for falls among older adults. The second section presents human physical activity recognition by inertial measurement units (IMUs). Specifically, the support vector machine (SVM) classifier, which is used as a tool for classifying fallers and non-fallers, are demonstrated theoretically. Additionally, the corresponding advantages and disadvantages of SVM classifier are further discussed. Finally, a literature review of different fall risk assessment approaches is presented, specifically inertial measurement units (IMUs) based methods are emphasized, since IMUs are used as experimental apparatus in this study.

2.1 Mechanisms of Gait and Fall

Human gait is defined as a continuous process of a person's body weight's transferring from one place to another [23]. Usually one gait cycle starts from the initial heel contact of the contacting foot and ends with the next consecutive heel contact of the same foot. One gait cycle usually contains two main phases: the stance phase and the swing phase. The stance phase is defined as the duration time when the foot is in contact with the ground, approximately from 0% to 60% of the gait cycle; and the swing phase is defined as approximately from 60% to 100% of the gait cycle [24]. Both these two phases could be further divided into several sub-phases. Based on Cochran's study [25], the stance phase could be divided into initial contact (0%), loading response (0-

10%), midstance (10-30%), terminal stance (30-50%), and preswing (50-60%); the swing phase could be divided into initial swing (60-70%), midswing (70-85%) and terminal swing (85-100%). A typical gait cycle is demonstrated in Figure 2-1.

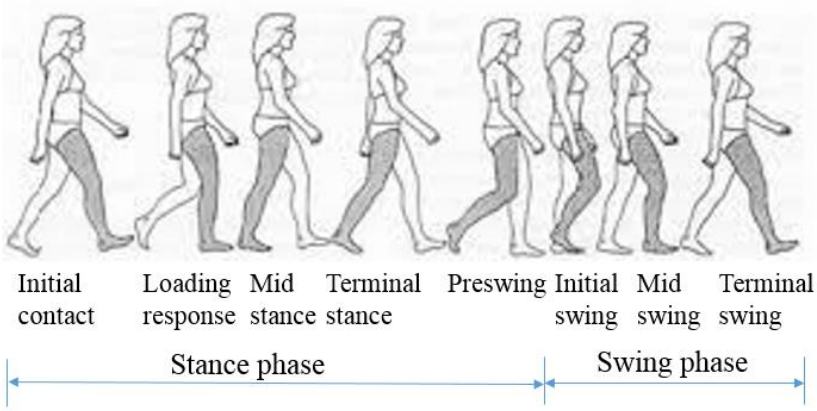

Figure 2-1: A typical gait cycle.

From biomechanical perspective, a gait cycle is assumed as a repeated process of balance loss and regain. The center-of-mass (CoM) of an individual's whole body is always outside the base of support except for the short duration time in double support phase [26]. However, the displacement of the whole body CoM could be well controlled within a range during normal gait cycle with the base of support, such as the sensory system, center nervous system, musculoskeletal system, etc. Therefore, though sometime one individual loses the local balance temporarily, he/she could modulate quickly during next stance phase. Consequently, global loss of balance may result from delayed or insufficient transition of the whole body CoM [21].

As for a "fall," it is defined as "unintentionally coming to the ground, or some lower level not as a consequence of sustaining a violent blow, loss of consciousness, sudden onset of paralysis as in stroke or an epileptic seizure" [27]. Based on Lockhart's study, a fall could be divided into three phases: initiation, detection, and recovery [15]. Falls are caused by complex interactions between intrinsic risk factors and external risk factor, which would be discussed in the next section.

2.2 Falls Risk Factors

As discussed previously, falls usually cause physical suffering and functional impairments to the individuals, but also bring increasing medical cost and absenteeism in the work places. Fall risk factors can be identified by two categories: intrinsic or extrinsic risk factors.

2.2.1 Intrinsic risk factors

Many studies show that intrinsic risk factors of falls are mainly caused by many factors, such as decrease in range of motion and muscle strength, sensory loss, gait impairment, balance impairment, syncope, hemiplegia, hypotension, cardiac problems, progressive neurological disorders, side effects of medications, cognitive or perceptual impairment, vertigo, or any disease state that may influence mobility and stability [11]. Usually these factors are unchangeable; however, they are manageable and controllable through various interventions.

2.2.1.1 Musculoskeletal system

The musculoskeletal system is responsible for maintaining balance, and it declines as a person ages. The symptom of degraded musculoskeletal system, such as muscle atrophy, calcification of tendons and ligaments, increased curvature of the spine, etc., all affect balance [11].

Complex changes in muscle properties take place as a person ages. Muscle force production and muscle strength decreases with aging, which may influence the initiation of slip-induced fall accidents, and the recovery ability from slips and falls [11]. Aging would also lead to reduction of the total skeletal muscle mass, which is another main cause of the age-related decrease in muscle strength and power. It was reported that by 70 years old, the cross-sectional area of skeletal muscle is reduced by 30 to 40% [19]. According to performance and biochemical characteristics of individual muscle cells, muscle fibers could be divided into two different types: type I (slow-twitch) and type II (intermediate or fast-twitch). Fast twitch muscle fibers (type II) degrade faster than slow twitch muscle fibers (type I) [28]. It was found that decrease of the size of type II muscle fibers inhibits fast recovery from falling and slipping [29]; moreover, studies have reported that fallers have weaker lower limb muscles than non-fallers [30], and the elderly may fall more frequently due to the lower limb muscle weaknesses [31]. Do et al. claimed that one person’s reaction from loss of balance is based on his/her ability to generate explosive strength and control rapid, large-scale lower extremity motions [32]. The difficulty of older adults to utilize their joints and extremities to counterbalance the body’s horizontal momentum during recovery from falls, could explain the phenomenon of the increased frequency of fall accidents among the elderly. Numerous studies support this hypothesis by demonstrating that the high frequency of falls is caused by the declines in both voluntary muscle strength and rates of muscle force production.

2.2.1.2 Vision

Visual system plays a vital role in posture stabilization, locomotion guidance and slip response control by continually updating information to the central nervous system (CNS) [15, 33]. Changes of vision with age are considered as another significant cause of fall accidents. Many factors could increase the occurrence of falls, such as the difficulty to see obstacles in one's path, changes in surface conditions, and obstacles such as stairs or ramps.

Vision changes with age. An older person usually requires three times of light and color contrast to see the object clearly compared to a younger person. This deficit in vision increases a person's risk for falling. Tinetti et al. stated that vision is important in controlling stability, both in standing still and ambulating [33]. Many factors of vision declines with age, such as visual acuity, ability of accommodating to the dark environment, peripheral vision, contrast sensitivity, etc. Numerous studies focused on the influence of age-related changes on visual input during static activities such as standing [34-36]. Studies show that elderly people depend more on visual cues (e.g., the locations of stable surroundings) during static stability [35], whereas young people depend more on proprioceptive and vestibular cues [37]. Therefore, the elderly may pay more reliance on the spatial framework provided by vision in order to compensate for reduced vestibular and peripheral sensation [38].

It was found that the inability to maintain postural balance with age has close relationship with reduction in tendon stiffness and absence of visual input [35]. Declines of visual performance is usually related with age and visual deficits from common eye pathologies, such as cataracts, macular degeneration, glaucoma, etc., which are also associated with slips and falls in later life [39].

Additionally, as age increases, it will limit the gazing ability to look upwards because of physical limitations, such as arthritis of the neck, stoop posture, drooping eyelids, limited vertical eye movements [40]. Biomechanically, tilting the head will deviate the whole body COM outside of support base and decrease postural stability, which is considered as a factor associated with high risk of fall accidents.

2.2.1.3 Gait

Significant differences exist in gait between older and younger individuals [15]. Older adults tend to walk slower, maintain a shorter step length, and a broader walking base [21, 41]. Slower walking velocity could increase stance time and double support time for older adults to maintain the dynamic balance. In general, shorter stride length, broader walking base, and slower walking velocity are considered to result in a more stable, safer gait pattern. Studies show that slower walking velocity coupling with higher heel contact velocity among the elderly significantly increases fall risk comparing to the younger individuals [21].

Although gait adjustments are considered to be helpful for reducing horizontal foot force to improve gait stability in older adults, they still undergo slips and falls more frequently than younger adults. It was hypothesized that these gait adjustments may relate to the initiation of slip-induced falls. However, Lockhart et al. found that the likelihood of slip initiations is similar across all age groups [15]. Additionally, Lockhart et al. indicated that older adults have slower transitional acceleration of the whole body COM during ambulating, which may influence slip initiation and slip recovery [21].

Therefore, the acquisition of gait characteristics during walking could provide important information about limb propulsion and control, which may lead to insight into muscle performance. Furthermore, gait evaluations could be used as global indicators of stability, as well as an effective tool for evaluating and quantifying gait problems associated with fall-prone individuals.

2.2.1.4 Nervous system

Human balance depends on the multiple interactions from sensory, motor, and nervous system. All of these systems decline significantly with age; and these degradations are associated with fall accidents in the elderly. The nervous system has two components, the central nervous system (CNS) and the peripheral nervous system (PNS). Although both systems are separated anatomically, they are still interconnected and interactive [42]. The CNS plays significant roles in integrating the sensory inputs from multisensory neurons of different sensory systems, as well as adapting output to a continuously changing internal and external environment [42]. Obviously, age-related deterioration in the CNS affects goal-related sensory information integration, motor programs selection, and motor responses execution.

Sensory receptors play a critical role in creating effective movements by providing information from the external environment. Researchers have reported that sensory systems including visual, vestibular, and proprioceptive systems are all relevant to motor control and balance maintenance [15, 43]. The accuracy of CNS decision making depends on the accuracy of information obtained from these sensory systems, which have redundant and different operating frequency ranges that affect their influence on postural control in different situations [44].

The performance of these systems declines at the different rates [45]. It was indicated that sensory loss with age is the main reason for which older adults lose their orientational sense [46, 47]. Therefore, age-related deterioration in the sensory systems could decrease the redundancy of sensory inputs, in order to ensure stability while one or two inputs are lost.

Many other neurological conditions, such as Parkinson's disease, seizure disorder, paralysis, diabetic neuropathy, etc., also affect the balance and mobility of the elderly.

2.2.1.5 Cognition

Older adults experience more cognitive impairments and dementia as age increases. Older adults with dementia fall twice as often as older adults without cognitive impairment. Impaired gait characteristics and balance brought from dementia cause the higher rate of fall accidents. It was indicated that the elderly with an abnormal gait, which is usually one of characteristics of dementia, experience more fall accidents than the elderly without an abnormal gait and dementia [19, 41].

2.2.1.6 History of falls

Once an elderly person falls, the chance of falling again within a year increases dramatically. Unfortunately, researchers emphasize less on the influence of an individual's fall history on the subsequent falls, although it is reported as one of the strongest risk factors, particularly in studies conducted in long-term settings. Usually the causes of the subsequent falls are similar: the initial fall leads to restriction of activity, loss of autonomy and self-confidence, depression and anxiety, deconditioning, possible prescription of psychoactive drugs; therefore, after the initial fall accident, the risk of subsequent falling will increase. And this may explain the increased risk of falling in individuals who had the history of falls [19].

2.2.1.7 Other intrinsic factors

Other intrinsic factors, such as cardiac system, medications, influenza, urinary infections, pneumonia, etc., also could cause hypotension, syncope, and electrolyte imbalance resulting in weakness. In addition, any condition that causes an elevated temperature may also cause weakness and falls.

2.2.2 Extrinsic risk factors

The second category of fall risk is extrinsic risk factors. Extrinsic factors involve the environment surrounding the person, such as placement of furniture, existence of obstacles, use of assistive walking devices, lighting, stairs, or any other object in the person's environment that may put them at risk for falls.

2.2.2.1 Environment

Forty percent of the fall accidents in the elderly population involve environmental hazards [10]. Many factors in the environment can increase individual's fall risk. Glare on the floor, loose rugs, patterned carpets, and slippery floors are all problems for older adults who have poor eyesight and inability to recognize these hazards quickly. In addition, improper footwear could cause falls.

2.2.2.2 Appliances/devices

Various appliance and devices utilized by elderly residents can increase their risk for falling. The use of canes, walkers, and crutches increase the risk for falls if used improperly. These devices can get caught on loose rugs or small elevations on the floor surface and cause a person to fall.

In general, many intrinsic and extrinsic risk factors contribute to falls, which is summarized in Table 2-1. This study focuses on intrinsic risk factors. Specifically, the relationship between gait and postural parameters and fall risk was investigated.

Table 2-1: Summary of fall risk factors.

Intrinsic Risk Factors	**Extrinsic Risk Factors**
Musculoskeletal system	Environment
Vision	Appliances/devices
Gait	
Nervous system	
Cognition	
History of falls	
Other intrinsic factors	

2.3 Human Physical Activity Recognition

2.3.1 Inertial measurement units (IMUs)

An inertial measurement unit (IMU) is an electronic device which measures linear accelerations, angular velocities, orientation, and gravitational forces. An inertial measurement unit, or IMU, is a piece of miniature electromechanical device that measures linear accelerations, angular velocities and orientations [48]. An IMU usually consists of accelerometers, gyroscopes, and sometimes magnetometers. The accelerometer is used to measure the inertial acceleration, while gyroscope is used to measure angular rotation. Both sensors typically have three degree of freedom to measure from three axes. In 1930s, IMUs were first applied to the areas of aircraft guidance and navigation [49]. IMUs have limited application at that time due to its constraints in size, cost, and power consumption. Until recently, as the micro-electromechanical system (MEMS) techniques develop, IMUs have been widely used for human motion monitoring to estimate energy expenditure, recognize daily activities and characterize walking [50].

The accelerometer in IMUs is an instrument used to measure the acceleration acting along a sensitive axis [51]. Although the measures of acceleration have different types of mechanisms, such as capacitive, piezoelectric, piezoresistive, etc.; however, all of them use the variation of a spring mass system for acceleration capture [51]. Acceleration signals have been widely used in the areas of pattern recognition, event detection, time-frequency analysis, and biomechanical modeling [52].

A gyroscope in IMUs is used to measure the angular velocity with reference to a sensitive axis [50]. The principle is to utilize a rotating reference frame to achieve an apparent force, which is proportional to the angular rate of the rotation. Typically, gyroscopes utilize a vibrating mechanical system to obtain the vibration value by transferring the energy generated by the Coriolis force [53]. There are advantages and disadvantages for the gyroscopes. The major advantage is the robustness, which means the angular velocity could keep the same no matter where the gyroscope is attached on a body segment, as long as its sensitive axis is parallel to the axis of rotation [54]. While the drawbacks of gyroscopes are the requirements of more power consumption, higher price, more significant drifting problem, and being sensitive to shock, which limit the usability of this system [50]. Comparing to accelerometers, gyroscopes have not been widely applied in human motion monitoring; however, the promising features of gyroscopes may explore more applications for body movements and daily activity recognition [50].

A magnetometer is used to measures the strength and/or direction of the magnetic field in the vicinity of the instrument [55]. Magnetometers are usually used to evaluate sensor orientation [56], and the function of magnetometers is to correct the drifting of accelerometer or gyroscope signals, in order to increase the measurement accuracy [55].

In general, there are two different types of IMU, one type of IMU consists of accelerometer and gyroscope, as shown in Figure 2.3; and the other type consists of accelerometer, gyroscope and magnetometer, as shown in Figure 2.4.

Typically, each sensor has three degrees of freedom (DOF) defined for *x*, *y*, and *z* axis, thus the IMU containing accelerometer and gyroscope will total up to six DOF. Acceleration values obtained from accelerometer and angular velocity from gyroscopes are kept separately. Angles can be measured from both accelerometers and gyroscopes, so both of the data could be calibrated to generate output more accurately. The advantage of this type of IMU is that it will not be interfered by external magnetic field in the ferromagnetic environment. The drawback of this type of IMU is the dependence on accelerometer and gyroscope which may be inaccurate due to sensors' noise and the gyroscopes' drift issues.

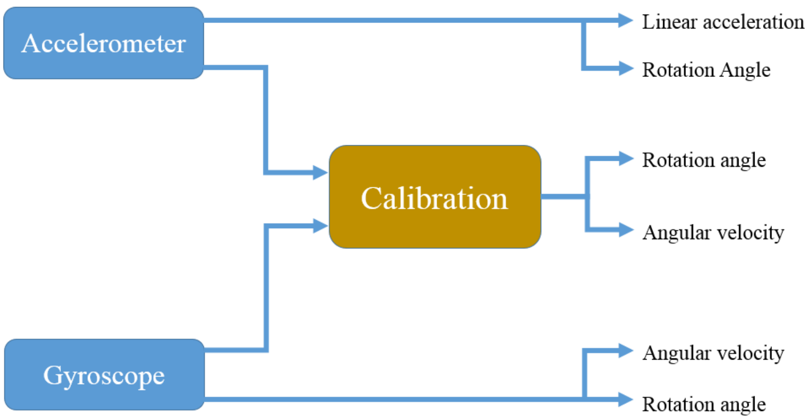

Figure 2-2: IMU consisting of accelerometer and gyroscope [57].

The other type of IMU, consisting of accelerometer, gyroscope and magnetometer, increases the DOF to nine. The magnetometer is used to measure yaw angle, thus it can be used to calibrate the gyroscopes' drift. This type of IMU is suitable for dynamic orientation calculation and has more accurate outputs. The disadvantage of this type of IMU is that the measurements might be affected due to the disturbance to magnetic field [58].

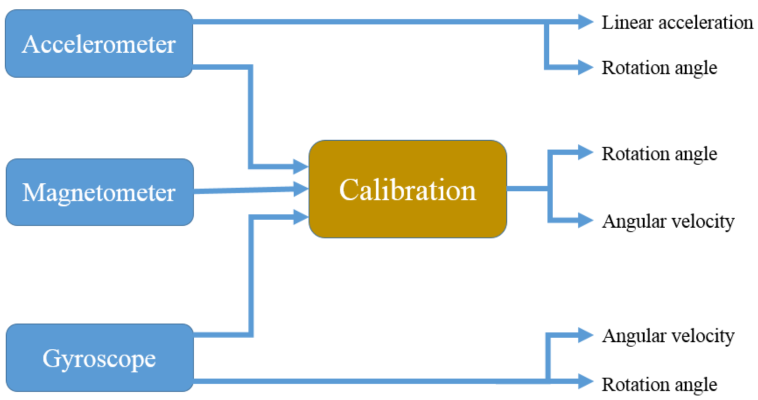

Figure 2-3: IMU consisting of accelerometer, gyroscope and magnetometer [57].

2.3.2 Physical activity assessment with IMUs

IMUs have many advantages for physical activity assessment such as noninvasive measurement, low burden for subjects, low cost, and so forth [51, 59, 60], comparing to traditional motion capture techniques. Assessment of physical activities is able to provide information about health conditions [61], including fall risk assessment. The application of IMUs in physical activity assessment can be categorized into three levels: energy expenditure estimation, activity recognition, and gait analysis.

2.3.2.1 Energy expenditure

Energy expenditure (EE) estimation is one of the applications that utilize IMUs to investigate physical activity assessment. The theoretical principle of EE is that accelerations are proportional to the muscular forces and thus are related to EE [62]. Typically, there are three approaches to calculate EE estimation. The first approach is to calculate the times that the acceleration signals cross a fixed threshold (zero or a certain value). The second method is to detect the maximum value for a selected time period as the calculation of times. The third and most commonly applied approach is to calculate the area under the acceleration curve (integration or average) [63, 64].

In the early 1980s, Wong et al. found out a rough linear correlation between the acceleration measurement and oxygen consumption by utilizing a waist-worn accelerometer device [65]. Montoye et al. found that the acceleration measurement has better reproducibility comparing to commercial movement counters [66]. Recently, numerous single or multiple, linear or nonlinear equations have been developed to estimate EE in physical activities. All of the equations would be applied to the different situations. The equations developed for locomotion activities (e.g. walking and jogging) usually underestimate the EE of lifestyle activities, which usually involve substantial upper body activities [67-70]; conversely, the equations developed for lifestyle activities overestimate the energy cost when they are applied to locomotion activities [68, 71].

To overcome this problem, different intensities or types of activity need to be identified, in order to make correct selection of different equations. One method is to utilize activity counts per minute to classify different types of activities, such as light, moderate, or vigorous activities, and then employ different models to estimate EE [72]. Another approach is to use the feature of coefficient of variation (CV) (standard deviation (SD)/mean) to distinguish locomotion and lifestyle activities, and then employ different models to evaluate EE [73-75].

2.3.2.2 Activity classification

IMUs have been widely used to identify types of physical activities by different classifiers [76]. Most studies have used multiple IMUs [77-82]; while some studies have used only one IMU attached to different locations of the body [83-90].

Classification of human physical activities in a free-living environment is an important aspect of many scientific investigations. There are numerous pattern recognition or machine learning approaches that are employed to address the problem of classifying human physical activities from IMUs. Activity classification is a recent concept involving the use of machine learning technology to automatically recognize different activities [82, 91]. The machine learning approaches have been widely applied to many fields, such as healthcare informatics [92, 93], network security [94, 95], natural language processing [96], as well as human physical activity recognition [82, 91].

2.3.2.2.1 Classifiers

The taxonomy of *classifiers* is explainable in different criteria [97]. First, classifier could be categorized into supervised and unsupervised classifiers [98-100]. In supervised classifiers, the training data is labeled, namely the categories of certain data are already known to the system in advance beforehand. A significant amount of labeled activity data is required in order to "train" the classification algorithm. Once the training process is complete, the classifier is able to assign an activity label to the unknown data. As for the unsupervised classifiers, only the number of classes is known, and then the system responds to the instances in the training set by assigning a label to each of them. Further, the classifiers can be divided into three different categories: probabilistic (such as naive Bayesian, logistic, Parzen and Gaussian Mixture Model (GMM) classifiers); geometric (such as Artificial Neural Networks (ANN), *k*-Nearest Neighbor (*k*-NN), Nearest Mean (NM) and Support Vector Machines (SVM) classifiers); and template matching.

In the process of activity classification, the classical cross-validation (CV) [98] is usually adopted to evaluate the accuracy of the system in two different ways: between-subject and within-subject evaluation. In the between-subject case, the classifier is first trained with data from all subjects except for a few subjects and then, tested with data from the excluded subjects. The accuracy is calculated by the proportion of correctly classified data sets across all activities. The process of excluding certain subjects and performing a train-test cycle is repeated until all subjects have involved in the testing datasets. The overall accuracy is then calculated as the average accuracy across all train-test cycles. If only one subject is used for the testing, then the process is called leave-one-subject-out CV. For within-subject evaluation, training is performed by picking up a portion of data for a specific subject, and testing is performed by the remaining samples of the same subject. This process is then repeated, each time using a different portion of the subject samples for testing. The overall accuracy is determined by the average of all the cycles for all available subjects.

Support vector machine (SVM) [101, 102] is a popular machine learning method which has shown to be successful in various applications including human physical activity recognition. In this dissertation, SVM will be adopted as a classifier to recognize human movements and distinguish fallers and non-fallers.

2.3.2.2.2 Support vector machines (SVMs)

The SVM is a statistical method which is introduced by Guyon and Vapnik [102, 103] that has been widely applied to different classification needs [104-106]. The idea of the SVM algorithm is to map the original data (usually low-dimensional space) to a high-dimensional space using nonlinear mapping by finding an optimum linear separating hyperplane, with the maximal margin in this higher dimensional space [102, 103].

The SVM is a principled approach to machine learning utilizing the concepts from the classical statistical learning theory [102, 107, 108] and exhibits good generalization of new data with a readily interpretable model. Additionally, the learning involves the optimization of a convex function (i.e., one solution). From the perspective of statistical learning theory, the motivation for considering a binary classifier SVM comes from the theoretical bounds on the generalization error. These generalization bounds have two important features: upper bound is independent of size of the input space, and the bound is minimized by maximizing the margin between the hyperplane separating the two classes and the closest data point to each class – called support vectors. Closest points are called support vectors because they support where the hyperplane should be located. That is, moving the non-support vectors will not shift the hyperplane, whereas moving the support vectors will shift the hyperplane (Figure 2-4).

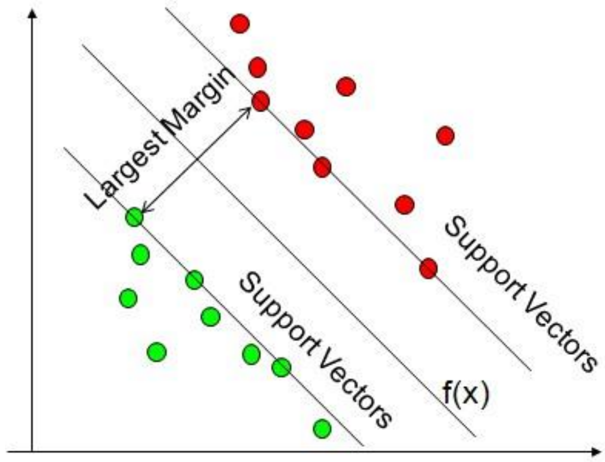

Figure 2-4: Linear support vector machine separation.

The basis of the SVM algorithm can be stated as follows: given a training data set: Θ, containing data feature vectors x_i and the corresponding data labels y_i, in the form of

$$\Theta = \{(x_1, y_1), (x_2, y_2), (x_3, y_3), \dots, (x_n, y_n) \qquad (2.1),$$

where $x_i \in \Re^m$, m is a dimension of the feature (real) vector, $y_i \in \{0, 1\}$, and n is the number of samples. We assume $g(x)$ is some unknown function to classify the feature vector x_i:

$$g(x): \Re^m \rightarrow \{0, 1\} \quad (2.2).$$

In SVM method, optimal margin classification for linearly separable patterns is achieved by finding a hyperplane in m dimensional space. The linear classifier is based on a linear discriminant function of the form,

$$f(x) = \sum_i w_i x_i + b \quad (2.3),$$

where the vector w_i is the weight vector and b is the hyperplane bias. While $f(x) = 0$ is called the hyperplane which separates the sampled data linearly.

In many cases, a linear classifier cannot satisfy the demand of accuracy due to its simplicity, thus a more sensitive classifier is needed for real-world applications. The intuitive idea of converting a linear classifier to a nonlinear classifier is to map the data from the input space to feature space using a nonlinear function:

$$f(x) = \sum_i w_i \phi(x_i) + b \quad (2.4),$$

where ϕ represents nonlinear feature mapping function: $x \in \Re^m$, $\phi(x) \in \Re^n$, and $n, m \in [1, \infty)$ reflects the mapping from data space to feature space. Thus, each data $\phi(x_i)$ would be corresponding to one element in feature space.

To achieve a nonlinear transform and avoid the problem of dimensionality, the kernel theory was introduced by implicitly mapping data from input space into higher dimensional space [101]. The kernel function $K(x, y)$ can be expressed as and is related to the $\phi\ (x)$ by,

$$K(x, y) = \phi(x)^T \phi(x) \quad (2.5).$$

The evaluation of a hyperplane in feature space is usually determined by the distance between the hyperplane and the training points lying closest to it, which are named support vectors (Figure 2-4). Therefore, it is necessary to search an optimal separating hyperplane to maximize the distance between support vectors and the hyperplane [101]. The distance from the hyperplane to a support vector is $\frac{1}{\|\boldsymbol{w}\|}$, thus we can get the distance between the support vectors of one class to the other class simply by using geometry $\frac{2}{\|\boldsymbol{w}\|}$.

As real life datasets may contain noise, an SVM can fit this noise leading to poor generalization – the effects of outliers and noise can be reduced by introducing a soft margin. The soft-margin minimization problem relaxes the strict discriminant by introducing slack variables, ξ_i and is formulated as:

$$\text{minimize } \Im(w) = \frac{1}{2}\sum_{i=1}^{l} w_i^2 + C\sum_{i=1}^{l}\xi_i$$
$$\text{subject to } \begin{cases} y_i(\sum_{i=1}^{l} w_i\phi(x_i) + b) \geq 1 + \xi_i \\ \forall i = 1 \dots l \end{cases} \qquad (2.6).$$

The Lagrange theory is applied to solve equation (1.6), and we can get the solved dual Lagrangian form of

$$\text{minimize } \Im(w) = -\frac{1}{2}\sum_{i=1}^{l}\alpha_i + \frac{1}{2}\sum_{i,j=1}^{l}\alpha_i\alpha_j y_i y_j K(x_i y_j)$$
$$\text{subject to } \begin{cases} 0 \leq \alpha_i \leq C \\ \sum_{i=1}^{l}\alpha_i y_i = 0 \end{cases} \qquad (2.7),$$

where $\alpha_1, \alpha_2, \dots, \alpha_l$ are the non-negative Lagrangian multipliers, and C is a constant parameter, called regularization parameter, which determines the trade-off between the maximum margin and minimum classification error.

Once we have found the Lagrangian multipliers α_i, then the optimal $\boldsymbol{w}^*$ can be obtained by:

$$\boldsymbol{w}^* = \sum_{i=1}^{n}\alpha_i\, y_i x_i \qquad (2.8).$$

Correspondingly, the value of optimal b^* can be derived from the constraints,

$$y_i(\langle \boldsymbol{w}, x_i \rangle + b) \geq 1 \qquad (2.9).$$

Thus, we can obtain the optimal b^* value:

$$b^* = -\frac{max_{y_i=-1}(\langle \boldsymbol{w}, x_i \rangle) + min_{y_i=1}(\langle \boldsymbol{w}, x_i \rangle)}{2} \qquad (2.10).$$

At this point, we have all of the necessary parameters to write down the decision function needed to predict the classification of a new data point x_{new}:

$$f(x_{new}) = sgn(\langle \boldsymbol{w}^*, x_{new} \rangle + b^*) = sgn(\textstyle\sum_{i=1}^{n} \alpha_i y_i \langle x_i, x_{new} \rangle + b^*) \qquad (2.11).$$

In essence, finding α_i and b^* and applying the choice of kernel into the decision function will classify new data points. In general, if α_i is non-zero - it is a support vector and, if α_i is zero - it is not a support vector. Intuitively, as illustrated in Figure 2-4, moving the non-support vector will result in no shift of the hyperplane (i.e., α_i is zero). The process of obtaining the quadratic program solution is known as training, and the process of using the trained SVM model to classify new data sets is known as testing.

SVMs have shown promising and effective results in handling small datasets, especially when the data is not regularly distributed or has an unknown distribution. But as with all classification techniques, SVMs have their advantages and disadvantages.

The advantages of the SVM technique can be summarized as follows: first, SVMs are capable of solving complex nonlinear classification problems by introducing the kernel trick. Therefore, the nonlinear classification problem in the original space can be solved linearly by mapping to the higher dimensional feature space. Correspondingly, computation complexity is efficiently decreased by using the dot products. Second, since the kernel implicitly contains a nonlinear transformation, no assumptions about the functional form of the transformation, which makes data linearly separable, is necessary. Moreover, the SVM algorithm does not rely on human expertise judgment beforehand, that means if the parameters C and γ are chosen appropriately, SVMs would still generate good results even when the training sample has some bias or noise. The robustness of SVMs will be discussed in detail in the following section. Because the optimization problem for SVM is convex, the solution is global and unique. This is an advantage compared to Neural Networks [109], which have multiple solutions associated with local minima and for this reason may not be robust over different samples. An interesting property is that the solution of the optimization problem is sparse. Many α_i values in the solution are equal to zero. In the dual space, the nonlinear SVM classifier takes the form

$$y(x) = sgn[\sum_{i=1}^{\#SV} \alpha_i y_i K(x, x_i) + b] \qquad (2.12),$$

where the sum is taken over the non-zero α_i values, which correspond to support vectors x_i of the training set. Hence, the obtained solution is sparse. Last but not least, the computational complexity of SVMs does not depend on the dimensionality of the input space, and there are restrict mathematical formulae to support SVM theory, thus this is another advantage compared to Neural Networks.

SVMs also have some drawbacks from a practical point of view. First, the most significant problem with SVMs is the high algorithmic complexity and extensive memory requirements in large-scale tasks. Another challenge for SVMs is the choice of the hyper-parameters and the kernel functions; selection of suitable parameters and kernel functions is crucial to the classification results. Finally, the SVM classifier is fundamentally a two-class binary classifier, which limits its applicability. Modifications are needed for addressing multi-class classification problems. Several improvements have been suggested to the original SVM algorithm in order to make them more robust in terms of generality, speed, and parameter selection [110-113]. One such algorithm is the least squares SVM (LS-SVM) algorithm introduced by Suykens et al. in 1999 [114]. The underlying idea in LS-SVMs is to modify Vapkin's SVM formulation [102] by adding a least squares term in the cost function. This variant circumvents the need to solve a more difficult quadratic programming (QP) problem and only requires the solution of a set of linear equations which lead to a significant reduction in the complexity of the solution.

2.3.2.2.3 Application on human activity recognition

There are numerous machine learning methods and models that have been applied for human activity recognition. Some researchers utilized threshold-based classification approaches to identify postural transitions by the change in segmental angles derived from either accelerometers [60] or gyroscopes [60, 115]. For example, Coley et al. utilized the peak angular velocity of the shank to differentiate stair ascent from level walking or stair descent [116]. And many studies have been conducted to differentiate between static postures and dynamic activity by only using the acceleration signals [117].

Fahrenberg et al. used a hierarchical method to recognize eight activities [118, 119]. Using the IMUs on the chest, wrist, shank and thigh of the participants, they were able to achieve almost 100% accuracy in the within-subject case, and 97% accuracy for the between-subject case [119]. Lee et al. applied similar method to differentiate five static and four dynamic activities by a single waist-mounted IMU [120]. Parkka et al. were able to recognize eight different dynamic activities by a threshold-based hierarchical classification scheme [121].

Decision trees have also been applied to physical activity classification [79, 86, 120]. Bao et al. recognized 20 activities with 86% accuracy by using five IMUs [80]. Maurer et al. investigated the performance of different features and classifiers to recognize six different human physical activities [122].

Foerster et al. were the first to utilize the *k*-NN approach to classify human physical activities [81]. They differentiated nine different activities in the within-subject case. Later, Foerster and Fahrenberg improved their method by combining a *k*-NN classifier with a hierarchical decision structure [123]. Therefore, they were able to accurately differentiate a wider range of activities than in their previous work [81]. Bussmann et al. used training data for each activity to specify a maximum and minimum value along each axis, so that they were able to achieve 89-93% accuracy for recognition [124].

Artificial neural network (ANN) is also used for human physical activity recognition. Zhang et al. used this approach to classify four different activities with more than 97% accuracy [125]. Other studies compared the accuracies from ANN method with those obtained with other classification approaches [78, 126-128].

Huynh and Schiele proposed a novel method by incorporating multiple eigenspaces with SVM algorithm, which demonstrated better performance comparing to a naive Bayes approach [129]. In another study, Krause et al. used an SVM classifier to recognize eight daily activities [130].

Researchers also utilized other machine learning classifiers to recognize human physical activities. For example, Lee and Lockhart proposed linear discriminant analysis (LDA) method to classify external load conditions during walking [131]. Pober et al. used a Gaussian Mixture Model (GMM) classifier to recognize four different activities [82]. Allen et al. also employed a GMM classifier to recognize several movements and postures [132]. Lester et al. utilized the hidden Markov model (HMM) to classify a number of daily activities [133]. Lee and Mase utilized fuzzy classifier to differentiate different movements [134]. Van Laerhoven and Cakmakci were the first to employ unsupervised learning techniques in activity monitoring [135]. Later, Krause et al. also used an unsupervised learning algorithm with multiple sensors for human physical activity recognition [136]. Table 2-2 summarizes human physical activity assessment methods with IMUs.

Table 2-2: Human physical activity assessment methods with IMUs.

Authors [ref.]	**Classifiers/methods**	**Results**
Coley et al. [116]	Threshold-based classification	Differentiated stair ascent from level walking or stair descent.
Mathie et al. [117].	Threshold-based classification	Differentiated between static postures and dynamic activity.
Fahrenberg et al.	Hierarchical method	Recognized eight activities.

[118, 119]		
Lee et al. [120]	Hierarchical method	Differentiated five static and four dynamic activities.
Parkka et al. [121]	Threshold-based hierarchical scheme	Recognized eight different dynamic activities.
Bao et al. [80]	Decision trees	Recognized twenty activities.
Maurer et al. [122]	Decision trees	Recognized six different human physical activities.
Foerster et al. [81]	*k*-NN approach	Differentiated nine different activities.
Foerster and Fahrenberg [123]	Combined a *k*-NN classifier with a hierarchical decision structure	Differentiated thirteen motions and postures activities.
Bussmann et al. [124]	*k*-NN approach	Differentiated more than twenty postures and motions.
Zhang et al. [125]	ANN	Classified four different activities.
Huynh and Schiele [129]	Incorporated multiple eigenspaces with SVM	Classified six human physical activities.
Krause et al. [130]	SVM	Recognized eight daily activities.
Lee and Lockhart [131]	LDA	Classified external load conditions during walking.
Pober et al. [82]	GMM	Recognized four different activities.
Allen et al. [132]	GMM	Recognized three postures and five movements.
Lester et al. [133]	HMM	Classified eight daily activities.
Lee and Mase [134]	Fuzzy classifier	Detected transitions between preselected locations and differentiate sitting, standing, and walking behaviors.
Van Laerhoven and Cakmakci [135]	Unsupervised learning classifier	Recognized seven different activities.
Krause et al. [136]	Unsupervised learning classifier	Achieved human physical activity recognition.

2.3.2.3 Gait analysis

Gait analysis is another aspect of applications using the IMUs in physical activity assessment. Willemsen et al. used accelerometers to detect critical events during a gait cycle with accelerometers [137]. Afterwards, numerous gait analysis using the IMUs have been extensively investigated. Tong et al. assessed gait parameters mounted on the shank and the thigh [54]. Aminian et al. used accelerations to detect phases in a gait cycle [138]. Generally, IMUs are able to provide satisfying estimation of gait parameters [139].

2.4 Technologies for Fall Risk Assessment

Although much has been learned about the mechanism of risk factors which contribute to fall accidents, fall accidents still remain as a significant problem associated with older adults. Numerous studies have proposed fall risk assessment tools which were developed to identify at-risk populations and guide intervention by highlighting remediable risk factors for falls and fall-related injuries [28]; however, most of the approaches fail in reducing the risk of falls and resultant injuries significantly [21]. This is due to the time between onset of a fall event and administrating fall intervention approaches [22]. The following are the methodological approaches currently used to assess fall risks among older adults.

2.4.1 “Check-lists” methods

Numerous risk factors have been investigated and identified, the available “check-lists” including all kinds of different fall risk factors are used to evaluate who among their residents are at high risk for falls. This approach is easy to use and implement; however, the reliability and validity of these measures are questionable [140, 141].

2.4.2 Forceplate for fall-risk assessment

One of the most relevant intrinsic factors for fall accidents is the ability to maintain static posture during standing. A decrease in the quality of balance could be caused by additional fall-risk factors, such as visual, vestibular or proprioceptive problems, etc. Therefore, postural stability is commonly used to identify the balance problems in elderly group. The main method for evaluating balance is to use a forceplate (FP) to analyze the sway [142]. The FP technique is one of approaches that have been widely applied in assessing postural stability in a quantitative way. The principles of measurement are based on the ground reaction forces generated by a body standing on or moving across; specifically, forceplate measure the three-dimensional components of the single equivalent force applied to the surface and its point of application (Center of Pressure, CoP).

Recently, numerous studies have been focused on FP-based assessment of fall risk. Based on Piirtola's studies, they found certain parameters from FP data may have predictive values for subsequent falls, especially various indicators of the lateral control posture [143]. Hewson et al. proposed discriminant model to find the trade-off between sensitivity and specificity [144]. Bigelow et al. utilized logistic regression to classify fallers and non-fallers in the elderly group [145]. Some researchers utilized the parameter of CoP velocity with eyes closed as the indicator [146-148], they found fallers have higher values comparing to non-fallers. Thapa et al. found fallers have higher sway area [149]. Bergland et al. found higher medio-lateral (ML) sway amplitude could be used as the indictor for the fallers [150]. Swanenburg et al. [151] utilized root mean square (RMS) of ML CoP sway area with eyes open as the indicator, and Shin et al. [152] uses ML CoP velocity with both eyes open and closed to identify the fallers. The recent studies which found fall-related outcomes associated with parameters of forceplate are summarized in Table 2.3.

Table 2-3: Brief review of forceplate-based fall risk assessment studies.

Authors [ref.]	**Methods or Parameters**
Hewson et al. [144]	discriminant function model
Bigelow et al. [145]	logistic regression
Boulgarides et al. [146]	CoP velocity with eyes closed
Maki et al. [147]	CoP velocity with eyes closed
Stel et al. [148]	CoP velocity with eyes closed
Thapa et al. [149]	sway area
Bergland et al. [150]	medio-lateral (ML) sway amplitude
Swanenburg et al. [151]	root mean square (RMS) of ML CoP sway area with eyes open
Shin et al. [152]	ML CoP velocity with both eyes open and closed

2.4.3 IMUS for fall-risk assessment

IMU technologies have also been widely accepted for the assessment by measuring activity level, posture transitions, static and dynamic stability, and spatio-temporal gait characteristics [20, 115, 153, 154]. Traditionally, researchers mainly focus on several tasks: postural stability (PS) with different test conditions (eyes open (EO), eyes closed (EC)) [155-158], sit-to-stand (STS) [115, 159], timed up and go (TUG) test [160-164] and normal walking (NW) velocity [163, 165, 166]. Usually, the TUG test is the most common task, since it contains both a transfer (STS) phase and a walking phase, so that it could provide information about balance (STS) and gait. Table 2-4 summarizes the IMU-based fall risk assessment studies.

Table 2-4: Brief review of the IMU-based fall risk assessment studies. (SP represents specification, SE represents sensitivity, and ρ correlation coefficient.)

Authors [ref.]	**Tasks**	**Approaches**	**Results**
Najafi et al. [118]	STS	Wavelet transform	SP≥0.95; SE≥0.95
Giansanti et al. [155]	PS with EO and EC	Statistical clustering	SP≥0.93; SE≥0.94
Giansanti et al. [156]	TUG	Multi-layer perceptron neural network	SP≥0.88; SE≥0.87
Gietzelt et al. [160]	TUG	Decision tree	SP=0.91; SE=0.89
Marschollek et al. [161]	TUG	Decision tree	SP=1.00; SE=0.58
O'Sullivan et al. [157]	PS with EO and EC	t-test	Significant difference
Greene et al. [162]	TUG	Logistic regression	SP=0.76; SE=0.77
Narayanan et al. [158]	TUG	Linear least squares model	ρ =0.73
Liu et al. [159]	SS and TUG	Linear least squares model	ρ =0.99
Bautmans et al. [165]	NW	t-test	SP=0.78; SE=0.78
Caby et al. [166]	NW	Feature selection	SP=1.00; SE=0.93
Marschollek et al. [163]	TUG and NW	Logistic regression	SP=0.58; SE=0.78
Weiss et al. [164]	TUG	Binary logistic models	SP=0.82; SE=0.87

Chapter 3 STUDY I: EFFECT OF GAIT AND POSTURAL PARAMETERS ON FALL RISK

3.1 Objective

The objective of this study was to investigate the relationship between gait, postural parameters and fall risk. Two groups of individuals, fallers and non-fallers, were recruited to analyze the differences in gait and postural parameters. Any individual who experienced a fall in the past four months was defined as a faller; individuals who did not fall in the past four months were defined as non-fallers.

It was hypothesized that gait and postural parameters are significantly different between fallers and non-fallers.

3.2 Methods

3.2.1 Subjects

Thirty community dwelling elderly persons, 19 females and 11 males, from Northern Virginia participated in this study. Fifteen of the older adults were fallers, and fifteen of them were non-fallers. All of the participants should have good health conditions, thus the exclusion criteria include cardiovascular, respiratory, neurological, and musculoskeletal problems, which had been checked for the participants before the experiments. The data was collected at a local senior center. All participants signed an inform consent form approved by the Institutional Review Board (IRB) at Virginia Tech prior to the inception of data collection. Participants willingly volunteered to participate in this experiment and no compensation was provided. Table 3-1 summarizes the demographic information of the study participants.

Table 3-1: Characteristics of the study sample (M+SD).

	# Males	# Females	Age (years)	Height (cm)	Weight (kg)
Fallers	10	5	79.2±6.4	166.9±9.6	83.2±15.1
Non-fallers	9	6	77.4±8.24	164.2±7.64	78.0±20.8

3.2.2 Apparatus

Participants wore three Inertial Measurement Unit (IMU) nodes [167], one is located at sternum level and the other two are located on lateral sides of right and left shank (Figure 3-1). The IMU node consisted of MMA7261QT tri-axial accelerometers and IDG-300 (*x* and *y* plane gyroscope) and ADXRS300, *z*-plane uniaxial gyroscope aggregated in the TEMPO [167] platform (Technology-Enabled Medical Precision Observation which was manufactured in collaboration with the research team at the University of Virginia). The data acquisition was carried out using a Bluetooth adapter and Laptop through a custom built LabView VI. Data was acquired with a sampling frequency of 128Hz. This frequency is largely sufficient for human movement analysis in daily activities which occurs in low bandwidth [0.8-5Hz] [168]. The data was processed using custom software written in Matlab (the Mathworks, Inc.) and libSVM toolbox [169].

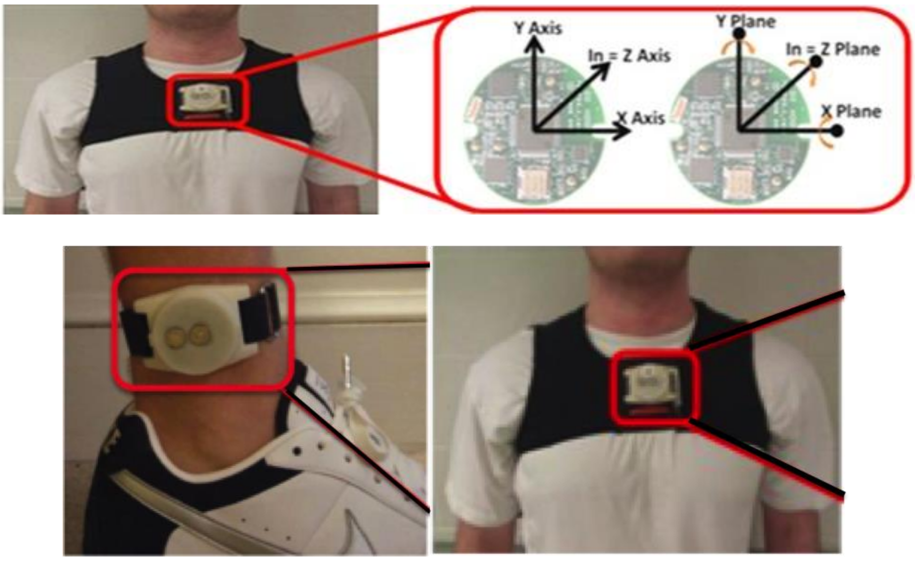

Figure 3-1: Picture of sensor located on one participant.

3.2.3 Experimental protocols

First, participants were instructed to walk at their own preferred walking pace. They were allowed to use their walking aid or cane. All participants were instructed to lift their dominant foot first in each trial. After that, the participants were asked to stand comfortably on the floor and the position of the feet was marked so that initial foot position remained constant across all trials.

Subsequently, participants were asked to perform a sit-to-stand (STS) task. The participants sat comfortably on a chair (with backrest and arm-rests) with their thighs and feet parallel, and then were instructed to use the armrests for support while performing STS task. The spacing between the feet was maintained at about 15 cm. A chair with 45 cm height (approximate height of popliteal) was used, and knee angle was maintained from 85°-90° by using a mat. Participants were then instructed to sit keeping the thighs apart from the seat, only with their buttocks rested on it. Afterwards, participants were asked to wait for an auditory signal before starting the task. The data was recorded for 6 seconds in total. The participants were given an auditory signal to stand after at least 2 seconds of data collection, in order to ensure sitting, postural transitions, and stabilized standing was collected in all trials [170]. Participants were then asked to perform the STS task twice using arms on the arm-chair from the previously defined sitting position.

The participants then were asked to perform a sit-to-walk (STW) test. The STW test has been widely used to investigate functional mobility among elderly individuals. The advantage of the STW test is the high reliability and validity. All participants were given verbal instructions and then demonstrated how the test should be performed. They sat comfortably in the same chair as the STS task, with their thighs and feet parallel. The participants were asked to wait for an auditory signal before initiating movement. They were then instructed to rise from the chair (either knee or arm support), walk at their self-selected pace to a target 3 meters away from the chair. The timing started when subject's back left the backrest of the chair, and stopped when the person's buttocks touched the seat again.

Finally, the participants were asked to stand still for 60 seconds for the measurement of postural stability. One trial was collected for each eyes open and eyes closed condition, respectively. TEMPO data was collected during the whole process. For the STS and postural stability task, only one IMU located at the sternum was used to collect data, since it allows for the movement of the whole body to be tracked [171]. While for the normal walking and STW task, three IMUs – one located at sternum, and the other two located at the right and left shank – were utilized to track the motion of the lower extremities [171].

3.2.4 Data analysis

The data was processed using custom software written in Matlab (MATLAB version 6.5.1, 2003, computer software, The MathWorks Inc., Natick, Massachusetts).

3.2.4.1 Signal denoising

Empirical Mode Decomposition (EMD) [172, 173] is a data-driven, adaptive signal processing technique, and can adaptively decompose the IMU signals, which could be considered as a time series, into different intrinsic mode function (IMF) components according to different time scales. And noise usually concentrates in the high-frequency components, namely the low level IMFs.

$$x(t) = \sum_{j=1}^{N} IMF_j(t) + r_N(t) \qquad (3.1).$$

The IMF should satisfy two conditions: 1) the number of extrema and the number of zero crossings must either equal to each other or differ at most by one, and 2) at any point, the local average is zero. The purpose of defining the two conditions is to allow for physically meaningful instantaneous frequency and amplitude calculation through the Hilbert transform performed on the IMFs. The symbol $r_N(t)$ represents the residue of the decomposition process, and is usually a constant or a function with only one extremum.

In the EMD process, a sifting algorithm is used to extract the IMFs from the original signal. Specifically, the upper envelope $e_{max}(t)$ and lower envelope $e_{min}(t)$ of the signal $x(t)$, are formed, based on the local maxima and minima of the signal through cubic spline interpolation, By defining the local mean of the upper and lower envelopes as $\frac{e_{max}(t)+e_{min}(t)}{2}$, the first component $h_1(t)$ is obtained as the difference between the signal $x(t)$ and the local mean:

$$h_1(t) = x(t) - \frac{(e_{max}(t)+e_{min}(t))}{2} \qquad (3.2).$$

This procedure is repeated until a pre-defined threshold is satisfied:

$$SD = \frac{\sum[h_1^{k-1}(t)-h_1^{k}(t)]^2}{\sum[h_1^{k-1}(t)]^2} < t_{th} \qquad (3.3),$$ where

t_{th} is usually within the range of 0.2 ~ 0.3. The final $h_1(t)$ is designated as the first IMF: $IMF_1(t)$. Subsequently the residue $r_1(t)$ is treated as a new signal and the sifting process is repeated until the residual $r_N(t)$ becomes a constant or a function with only one extremum such that no more IMF can be extracted. In the EMD representation of a signal, the lower-order IMFs correspond to fast oscillation components, while higher-order IMFs represent slow oscillations. If the EMD is interpreted as a time-scale analysis method, then the lower order and higher order IMFs correspond to the fine and coarse scales, respectively.

Ensemble Empirical Mode Decomposition (EEMD), is another approach which consists of sifting an ensemble of white noise-added signal and treats its mean as the true result [174, 175]. We used EEMD method to denoise on IMU signals. The number of ensembles chosen is 100 with ratio of standard deviation of the added noise to that of signal as 0.2, according to previous study [176].

3.2.4.2 Gait parameter computation

Walking Velocity (m/s): Walking velocity is defined as the distance covered by the whole body in a given time [177]. Thus the walking velocity (WV) could be obtained by:

$$Walking\ velocity = \frac{\text{Distance}}{t} \quad (m/s) \qquad (3.4),$$

where t represents the time of completing the distance of normal walking.

Gait Cycle Time (s): It is defined as the time interval between the exact same repetitive events of walking [177].

Double Support Time (s): It is defined as the amount of time during gait when both limbs are touching the ground at the same time, occurs at the very beginning and the very end of each gait cycle [178].

Right Stance (s): It refers to the time of right limb in contact with the floor [178].

Left Stance (s): It refers to the time of left limb in contact with the floor [178].

Mean Right Swing (s): It refers to the mean time of right limb not in contact with the floor [178].

Mean Left Swing (s): It refers to the mean time of left limb not in contact with the floor [178].

Step Length (m): The linear distance in the direction of progression between successive points of foot-to-floor contact of the first foot and other foot was measured on both floor surfaces. The step length was calculated from the difference between consecutive positions of the heel contacting the floor (resultant) using the general distance formula [15].

Cadence (steps/min): It refers to number of steps per minute [178].

3.2.4.3 Sit-to-Stand (STS) parameter computation

STS is a simple method for measuring lower limb strength and fall risks. STS is a regular mobility related activity in the daily life. Research has demonstrated STS parameters can provide significant indicator for the overall functioning and balance performance of older adults [179, 180]. Based on Etnyre and Thomas's study [181], STS can be divided into six event according to the vertical ground reaction force: (1) initial force change, (2) a counter force, (3) seat-off, (4) peak vertical force, (5) post-peak rebound, and (6) steady standing force. All of these events are divided from the aspect of forceplate.

From the view of IMU data, the STS could be divided into five events: (1) initiation, (2) peak flexion angular velocity, (3) seat-off, (4) peak extension angular velocity, (5) termination. Figure 3-2 illustrates the entire process of performing the STS task.

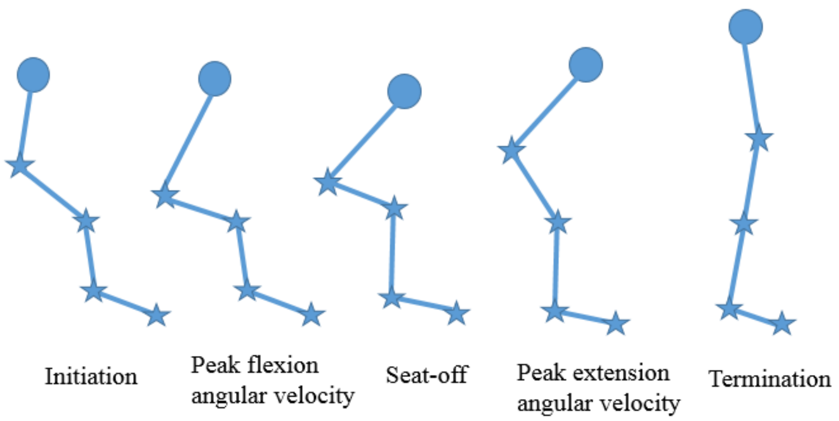

Figure 3-2: STS Events identified by IMU data.

The event identification was based on the IMU signals. And the special epochs from accelerometer and gyroscope provide the determination of events. The event of initiation (event 1) is defined as the start point of increase of angular velocity from gyroscope data. Angular velocity is absolute value from event 2 to event 3. Therefore, peak flexion angular velocity (event 2) is defined as the maxima, and peak extension angular velocity (event 4) defined as the minima. The event of termination (event 5) is defined as the end point of angular velocity. All of the four events are demonstrated in Figure 3-3 (a). The event of seat-off (event 3) is defined from the accelerometer data, namely the minima of the acceleration, which is shown in Figure 3-3 (b). In general, the gyroscope data was used to determine trunk flexion and extension angular velocities; while the accelerometer data was used to determine anterio-posterior (AP) accelerations. In addition, the peak-to-peak (P2P) acceleration (P2P_AP_Acc_Seat-off) can be defined in two ways: one is defined from AP acceleration initiation (event 6) to seat-off (event 3); the other way is from seat off (event 3) to AP acceleration termination (event 7). P2P_Flex/Ext_Ang_Vel is defined as the absolute value from peak flexion angular velocity (event 2) to peak extension angular velocity (event 4).

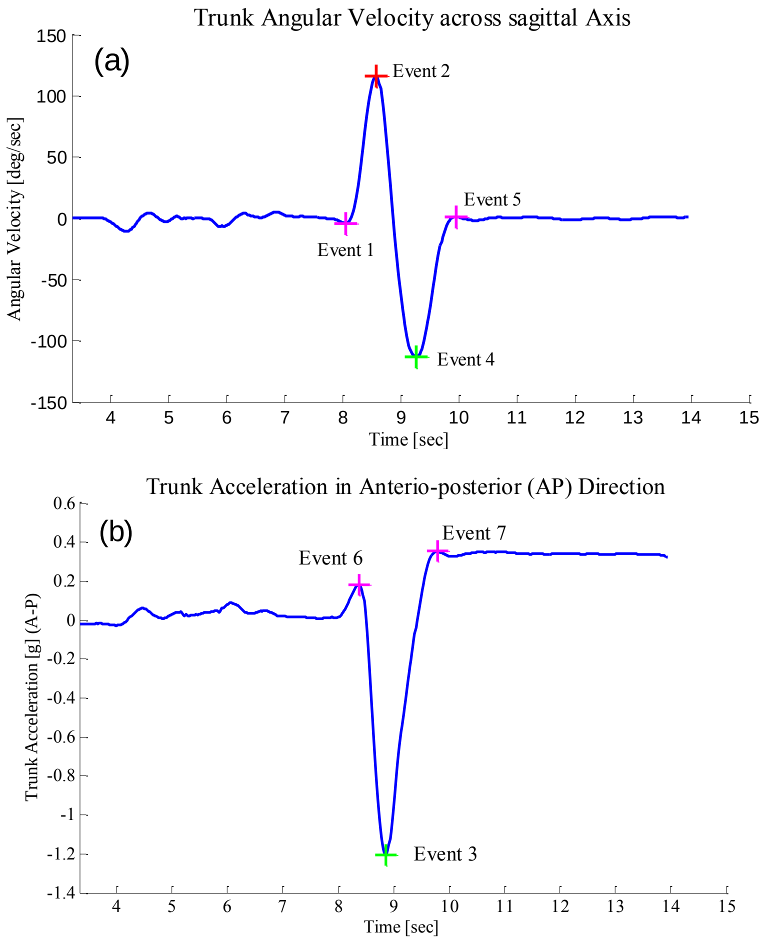

Figure 3-3: STS events identified by IMU data. (a) Trunk angular velocity with events (1. STS Initiation; 2. Peak flexion angular velocity; 4. Peak extension angular velocity, 5. STS termination); (b) Trunk acceleration with events (3. Seat-off; 6. AP acceleration initiation; 7. AP acceleration termination).

There are some other parameters that could be extracted from gyroscope data by STS task. For example, initial flexion angular acceleration (Initial_Flex_Ang_Acc) is calculated by the slope of angular velocities from event 1 (initiation of angular velocity) to event 2 (peak flexion angular velocity); late extension angular acceleration (Late_Ext_Ang_Acc) is determined by the slope of angular velocities from event 4 (peak extension angular velocity) to event 5 (termination of angular velocity). Similarly, pre-seat-off flexion angular deceleration (Pre_Seat-off_Flex_Ang_Dece) is identified by the slope from event 2 (peak flexion angular velocity) to event 3 (seat-off); while post-seat-off extension angular acceleration (Post_Seat-off_Ext_Ang_Acc) is calculated by the slope from event 3 (seat-off) to event 4 (peak extension angular velocity).

3.2.4.4 Sit-to-Walk (STW) parameter computation

From the IMU signals, the STW task can divided into eight different events: (1) initiation of STW; (2) peak flexion angular velocity; (3) seat-off; (4) peak extension angular velocity; (5) swing toe-off; (6) swing heel strike; (7) stance toe-off; and (8) stance heel strike. Also, the STW task could be divided into three phases: (1) flexion momentum phase; (2) combined extension and unloading phase; and (3) stance phase and eight postural transition and gait events detected. All of these events are shown in Figure 3-4. To identify these events, three IMUs located at the sternum and both shanks are required.

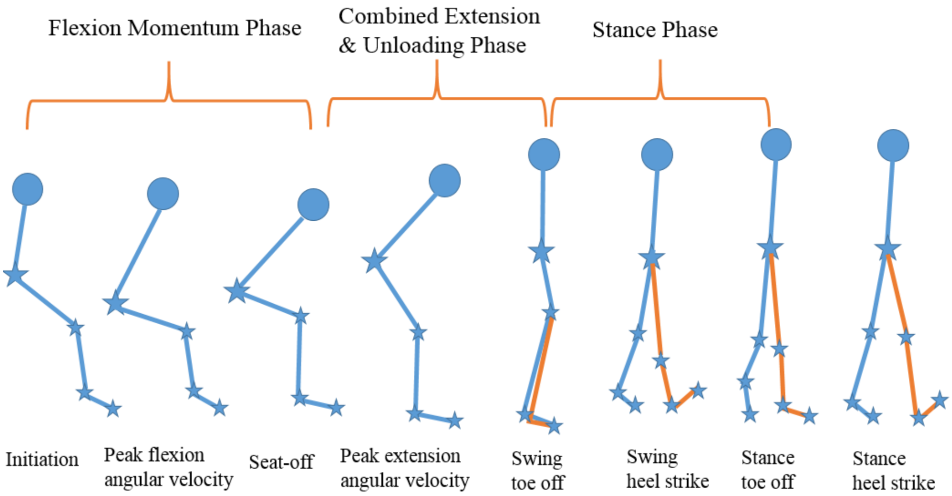

Figure 3-4: Three phases of the STW task: (1) flexion momentum phase; (2) combined extension and unloading phase; and (3) stance phase and eight postural transition and gait events detected.

The STW tasks include two phases: STS and normal walking. From the task of STW, numerous parameters could be extracted for fall risks assessment. Based on previous studies [182-185], gait cycle could be defined as a movement with the initial stepping leg designated as swing, and the second stepping leg designated as stance. According to the findings from Kerr et al. [183, 185] and Buckley et al. [182, 184], the STW task could be further divided into four phases: (1) flexion momentum phase; (2) extension phase; (3) unloading phase; and (4) stance phase. In their studies, they utilized a camera system and forceplate to evaluate center-of-mass (COM) vertical velocity and gait initiation (GI) event. In our study, only IMUs are used for analyzing data, which is void of kinetic information from the forceplate. Therefore, we combined the extension phase (phase 2) and unloading phase (phase

3) together. The other reason for combining these two phases is to avoid the conflicts on gait initiation event detection between the studies from Kerr et al. [196] and Buckley et al. [182]. Although the information of distinguishing the STS task and gait initiation is completely missing; however, the overall time for trunk extension phase and unloading phase can be easily evaluated using IMUs, so that it improves the robustness for this detection algorithm.

The first phase of STW task is the flexion momentum phase, and it includes three events: (1) initiation of STW; (2) peak flexion angular velocity; and (3) seat-off, as shown in Figure 3-4. During this phase, high flexion velocity is first generated, and then seat unloading is followed.

In the *x*-direction gyroscope signals from the IMU located at sternum, three events could be determined: event 1 (initiation of STW); event 2 (peak flexion angular velocity); and event 4 (peak extension angular velocity). Event 1 (initiation of STW) is identified as the first local maxima. And event 2 (peak flexion angular velocity) is defined as global minima, following event 1. In addition, the *x*-direction gyroscope signals are able to provide the information of event 4 (peak extension angular velocity): event 4 is defined as the second local maxima. Initial flexion angular acceleration of trunk is identified by fitting the slope from event 1 (STW initiation) to event 2 (peak flexion angular velocity event). All of these events are demonstrated in Figure 3-5.

Event 3 (seat-off) is determined from the z-direction acceleration signals from the IMU located at sternum. It is defined as the first local maxima, which is shown in Figure 3-6.

The second phase of STW is the combined extension and unloading phase. It comprises the extension velocity, momentary stabilization, gait initiation adjustments, and unloading. The events from 3 to 5 (seat-off, peak extension angular velocity, and swing toe-off) are included in the second phase. Event 5 can be detected from the gyroscope z-channel signals from the IMU located at left shank, which could provide enough information for the locomotion. It could be found by identifying the first local minima. Similarly, the event 6 (swing heel strike) is determined as the second minima in the same channel. These two events are shown in Figure 3-7.

The third phase is stance phase, which contains the events from 5 to 7. The identification of event 7 and 8 needs the gyroscope z-channel signals from the IMU located at right shank. Event 7 (stance toe-off) is defined as first local maxima, and event 8 (stance heel-strike) is determined as the second local maxima, which is illustrated in Figure 3-8.

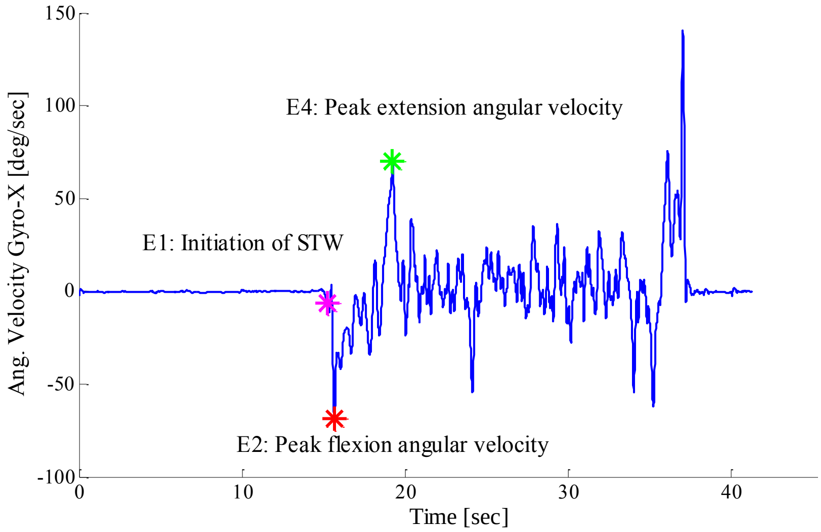

Figure 3-5: STW events identified by IMU data located at sternum: (1) initiation of STW; (2) peak flexion angular velocity; (4) peak extension angular velocity.

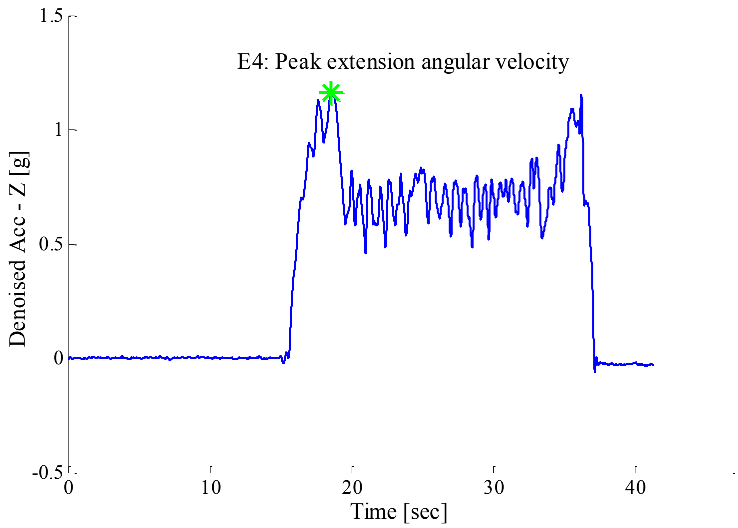

Figure 3-6: STW events identified by IMU data located at sternum: (3) seat-off.

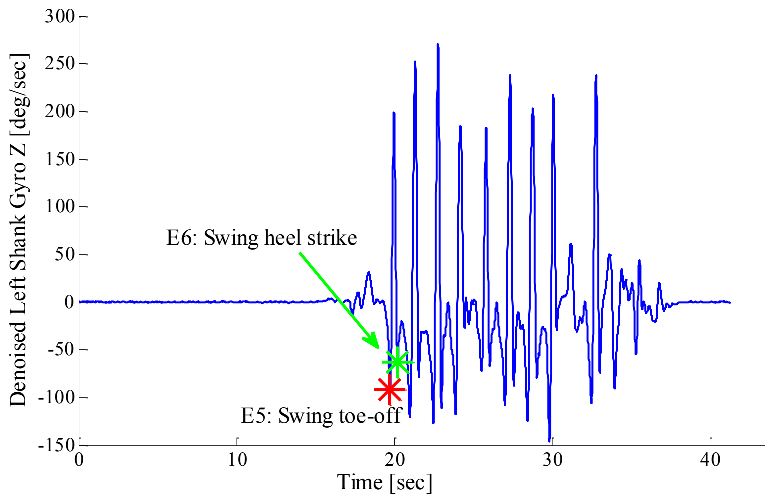

Figure 3-7: STW events identified by IMU data located at left shank: (5) swing toe-off; (6) swing heel strike.

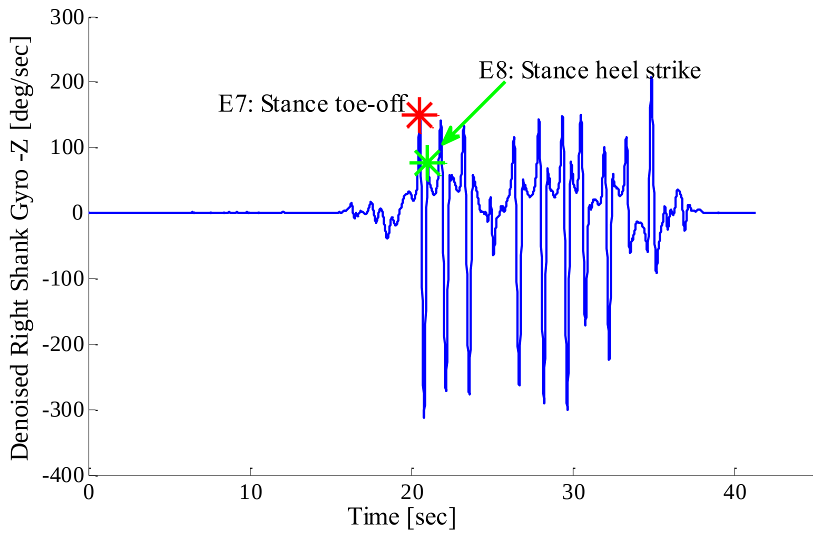

Figure 3-8: STW events identified by IMU data located at left shank: (7) stance toe-off; and (8) stance heel strike.

In summary, the gait and postural parameters could be extracted from normal walking, STS, and STW tasks, by three IMUs located at the sternum, and left and right shank.

3.2.4.5 Postural stability (PS) parameter computation

The trunk sway average velocity and mean radius recordings in the open eyes and closed eyes conditions were used for PS parameters.

The sway average velocity is defined by the path length (PL) over time. The PL is evaluated using the following expressions:

$$PL = \sum_{n=1}^{N} \sqrt{(x_n - x_{n-1})^2 + (y_n - y_{n-1})^2} \qquad (m) \qquad (3.5),$$

where (x, y) is the coordinate of ground projection of center of pressure (COP) from participants, and N is the number of data points. Thus, the sway average velocity can be defined as:

$$\text{sway average velocity} = \frac{\sum_{n=1}^{N} \sqrt{(x_n - x_{n-1})^2 + (y_n - y_{n-1})^2}}{60} \qquad (\frac{m}{s}) \qquad (3.6).$$

The mean radius is calculated by the formulation:

$$mean\ radius = \frac{\sum_{n=1}^{N} \sqrt{(x_n - \bar{x})^2 + (y_n - \bar{y})^2}}{N} \qquad (m) \qquad (3.7),$$

where (x, y) is the coordinate of ground projection of COP, (x_n, y_n) is the mean of all the (x, y) values, and N is the number of data points. Table 3-2 summarized all of the gait and postural parameters from the IMUs.

Table 3-2: Summarized parameters measured from the IMUs.

Type	Parameters
Gait	Walking Velocity
	Gait Cycle Time
	Double Support Time
	Right Stance
	Left Stance
	Mean Right Stance

	Mean Left Swing
	Step Length
	Cadence
Sit-to-Stand	P2P_AP_Acc_Seat-off [g]
	P2_Flex/Ext_Ang_Vel [deg/sec]
	Peak_Flex_Ang_Vel [deg/sec]
	Peak_Ext_Ang_Vel [deg/sec]
	Initial_Flex_Ang_Acc [deg/sec^2]
	Late_Ext_Ang_Acc [deg/sec^2]
	Pre_Seat-off_Flex_Ang_Dece [deg/sec^2]
	Post_Seat-off_Ext_Ang_Acc [deg/sec^2]
	t1_Peak_Flex [sec]
	t2_Seat-off [sec]
	t3_Peak_Ext [sec]
	t4_CompleteSTS [sec]
	t5_Initiation to Seat-off [sec]
	t6_Seat-off to Termination [sec]
	t7_Between Peak Flex./Ext. Momentums [sec]
	t8_Peak_Ext_Ang_Momentum to Termination [sec]
	t9_PeakFlexion to Seat-off [sec]
	t10_Seat-off to Peak Extension [sec]
Sit-to-Walk	P2P_AP_Acc_Seat-off [g]
	P2_Flex/Ext_Ang_Vel [deg/sec]
	Peak_Flex_Ang_Vel [deg/sec]
	Peak_Ext_Ang_Vel [deg/sec]
	Initial_Flex_Ang_Acc [deg/sec^2]
	Pre_Seat-off_Flex_Ang_Dece [deg/sec^2]
	Post_Seat-off_Ext_Ang_Acc [deg/sec^2]
	t1_ Peak_Flex [sec]
	t2_Seat-off [sec]
	t3_ Peak_Ext [sec]
	t4_Swing_TO [sec]
	t5_Swing_HS [sec]
	t6_Stance_TO [sec]
	t7_Stance_HS [sec]
	t8_Initital_Gait_Cycle [sec]
	t9_TotalSingleStance [sec]
	t10_GI_PartialDoubleSupport [sec]
	t11_ Between Peak Flex./Ext. Momentums [sec]
	t12_PeakFlexion to Seat-off [sec]
	t13_Seat Off to Peak Extension [sec]
	t14_Time_to_STW_Completion [sec]
Postural stability	Open Eyes Sway Velocity (m/s)
	Open Eyes Mean Radius (m)

Closed Eyes Sway Velocity (m/s)
Closed Eyes Mean Radius (m)

3.2.5 Statistical analysis

For testing hypotheses, subjects were first divided into two groups: fallers (F) group and non-fallers (N) group. A single-factor, fixed-effect, between-subject statistical model was established. The model can be expressed as:

$$Y_{ijk} = \mu + \alpha_i + \gamma_{j(i)} + \varepsilon_{k(ij)} \qquad (3.8),$$

where Y_{ijk} is a dependent variable (e.g. gait or postural characteristics), μ is the population mean of this variable, α_i is the effect of the between-subject factor being at level i, and γ_j is the random effect of subjects, $\varepsilon_{k(ij)}$ is the random error of a specific trial k.

Analysis of variance (ANOVA) tests were conducted for each experiment respectively. A significance level of $\alpha \leq 0.05$ was used. Two underlying assumptions of the ANOVA test were examined. The normality assumption was tested using the Shapiro-Wilk test. The homogeneity of variance assumption was tested using the Brown-Forsythe test.

3.3 Results

3.4.1 Gait parameters between fallers and non-fallers

Table 3-3 summarizes the results of gait parameters between the 15 fallers and 15 non-fallers. Figure 3-9 and Figure 3-10 provide the means and standard deviations of gait parameters and note significant difference between fallers and non-fallers.

Table 3-3: Results of gait parameters between fallers and non-fallers.

Gait parameters	**Fallers**	**Non-fallers**	**p-value**
Walking Velocity (m/sec)	0.83±0.13	0.84±0.10	0.3646
GC Time (Sec)	1.15±0.17	1.03±0.17	0.0352*
Double Support Time (sec)	0.27±0.10	0.18±0.07	0.0095*
Right Stance (sec)	0.66±0.08	0.60±0.11	0.0941
Left Stance (sec)	0.62±0.05	0.61±0.12	0.7676
Mean Right Swing (sec)	0.45±0.04	0.44±0.04	0.6779
Mean Left Swing (sec)	0.47±0.23	0.44±0.04	0.5090
Step Length (m)	0.45 ±0.07	0.43±0.08	0.5449
Cadence (steps/min)	110.41±19.83	117.95±16.33	0.1330

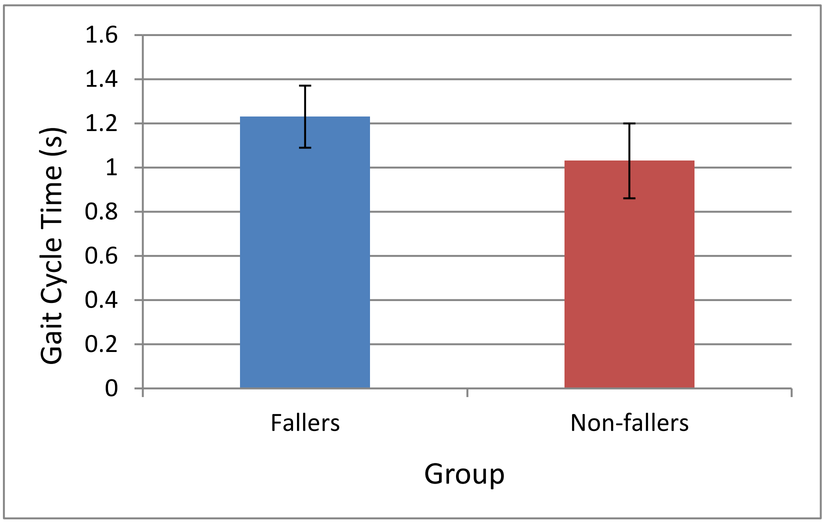

Figure 3-9: Means and standard deviations of gait cycle time for fallers and non-fallers.

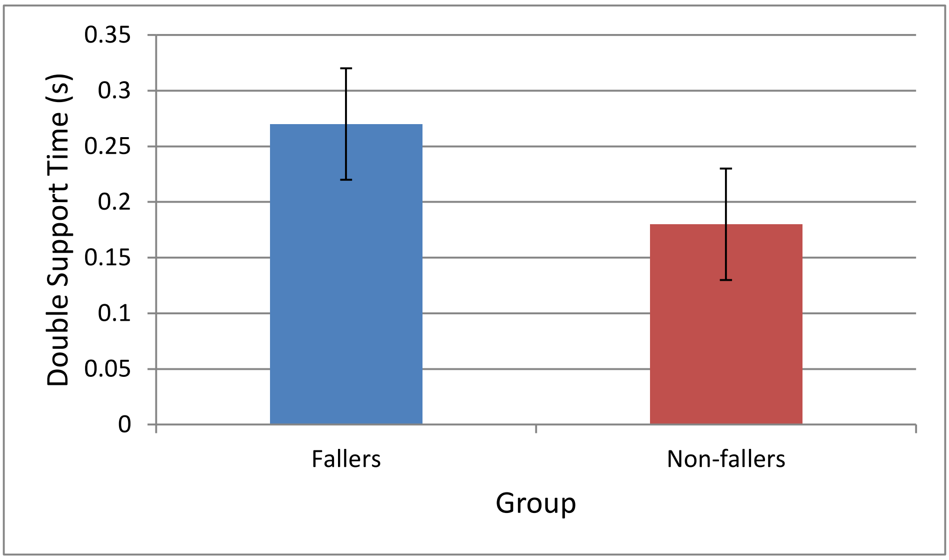

Figure 3-10: Means and standard deviations of double support time for fallers and non-fallers.

3.4.2 Sit-to-Stand (STS) parameters between fallers and non-fallers

Table 3-4 summarizes the results of the STS parameters between fallers and non-fallers. Specifically, five STS parameters were significantly different between fallers and non-fallers. Figure 3-11 shows the box-plot comparison of these parameters between fallers and non-fallers.

Table 3-4: Results of the STS parameters between fallers and non-fallers.

Sit-to-Stand parameters	**Fallers**	**Non-fallers**	**p-value**
P2P_AP_Acc_Seat-off [g]	1.09±0.28	1.23±0.29	0.1867
P2_Flex/Ext_Ang_Vel [deg/sec]	181.97±64.71	236.33±80.01	0.0503
Peak_Flex_Ang_Vel [deg/sec]	106.52±44.34	147.33±48.46	0.023*
Peak_Ext_Ang_Vel [deg/sec]	-33.37±40.23	-66.30±47.83	0.0508
Initial_Flex_Ang_Acc [deg/sec^2]	1.91±1.48	2.98±1.58	0.0666
Late_Ext_Ang_Acc [deg/sec^2]	0.63±0.34	1.55±1.33	0.0153*
Pre_Seat-off_Flex_Ang_Dece [deg/sec^2]	-2.46±2.74	-4.38±4.38	0.1622
Post_Seat-off_Ext_Ang_Acc [deg/sec^2]	-2.32±2.59	-4.53±3.72	0.0694
t1_Peak_Flex [sec]	1.44±0.43	1.01±0.35	0.0047*
t2_Seat-off [sec]	1.89±1.66	1.68±0.82	0.6618
t3_Peak_Ext [sec]	6.21±10.21	2.46±1.15	0.1681
t4_CompleteSTS [sec]	9.06±9.90	4.40±1.80	0.0467*

t5_Initiation to Seat-off [sec]	1.89±1.66	1.68±0.82	0.6618
t6_Seat-off to Termination [sec]	6.77±9.94	2.32±1.28	0.0967
t7_Between_Peak_Flex./Ext. Momentums [sec]	5.07±10.19	1.45±0.91	0.182
t8_ Peak_Ext_Ang_Momentum to Termination	2.44±0.80	1.54±0.71	0.0028*
t9_PeakFlexion to Seat-off [sec]	0.75±1.41	0.67±0.58	0.8551
t10_Seat-off to Peak Extension [sec]	4.62±9.88	0.78±0.69	0.1442

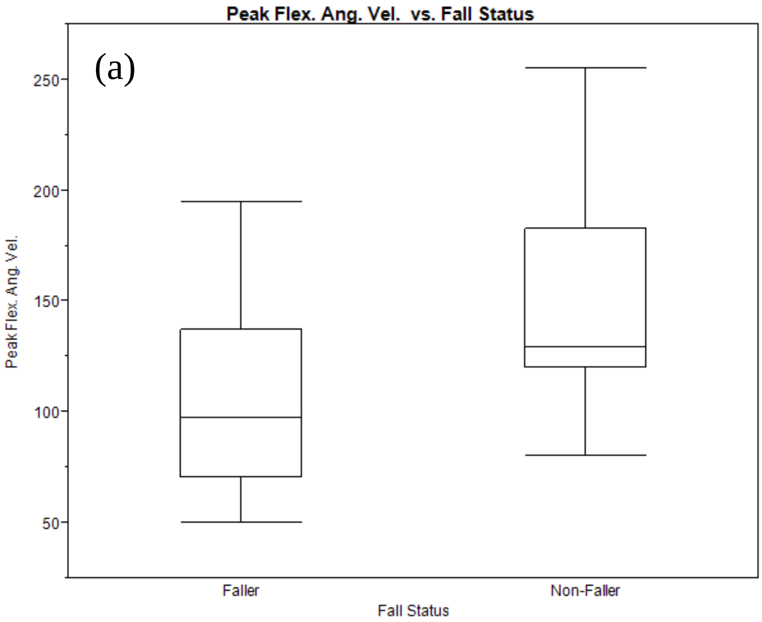

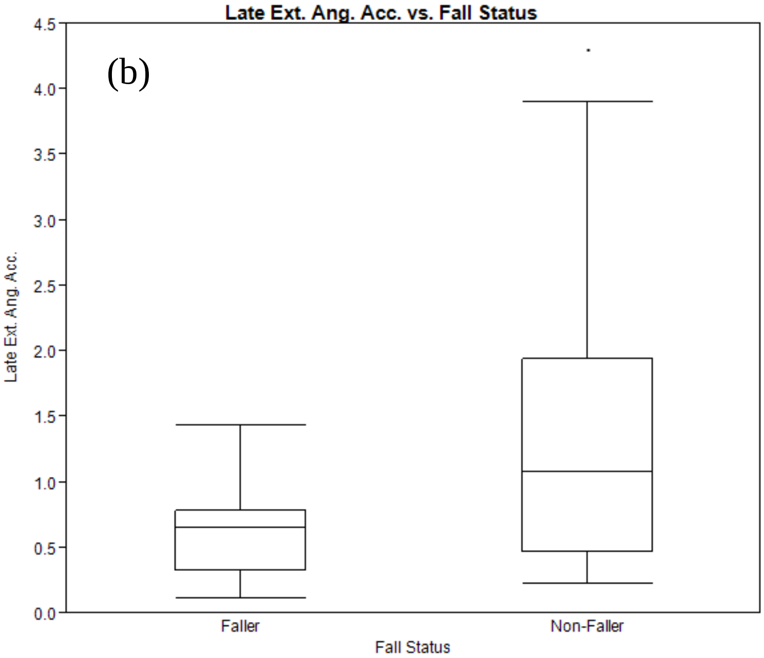

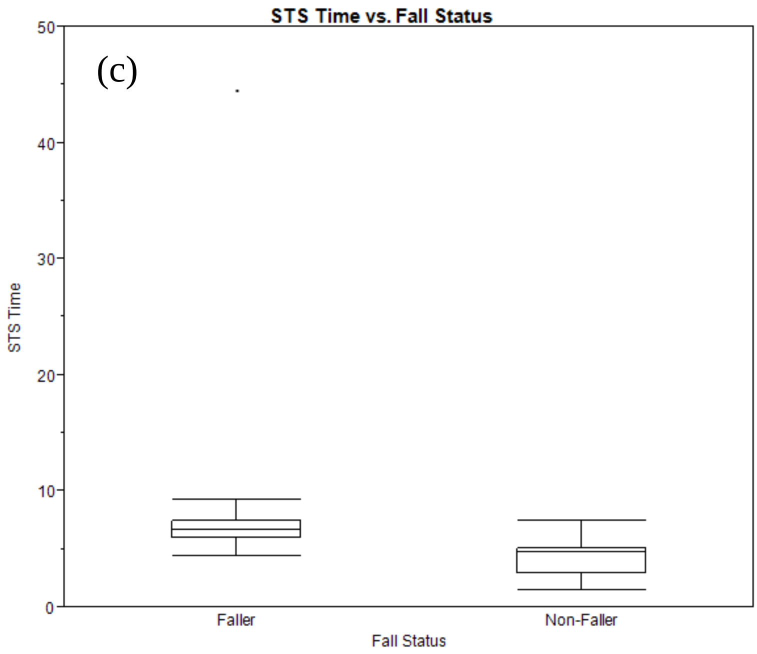
STS Time vs. Fall Status
(c)
50
40
30
20
10
0
STS Time
Faller
Non-Faller
Fall Status

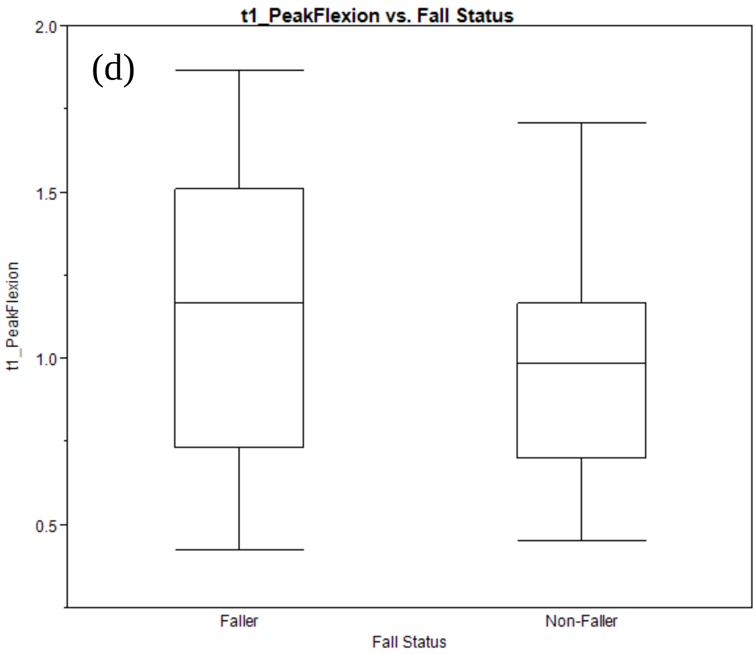
t1_PeakFlexion vs. Fall Status
(d)
2.0
1.5
1.0
0.5
t1_PeakFlexion
Faller
Non-Faller
Fall Status

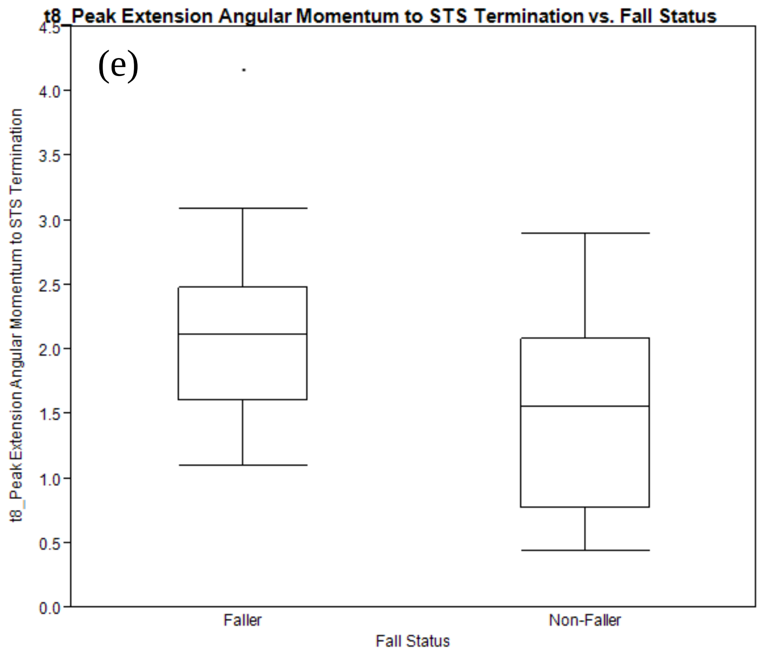

Figure 3-11: Box plots indicate five STS parameters which significantly differentiate fallers and non-fallers ($p < 0.05$): (a) Peak_Flex_Ang_Vel; (b) Late_Ext_Ang_Acc; (c) t4_CompleteSTS; (d) t1_Peak_Flex; (e) t8_ Peak_Ext_Ang_Momentum to Termination. The top and bottom of the box plot represent the first and third quartiles, and the middle bar indicates the median.

3.4.3 Sit-to-Walk (STW) parameters between fallers and non-fallers

Table 3-5 summarizes the results of the STW parameters between fallers and non-fallers.

Table 3-5: Results of the STS parameters between fallers and non-fallers.

Sit-to-Walk parameters	Fallers	Non-fallers	p-value
P2P_AP_Acc_Seat-off [g]	0.95±3.23	0.22±0.13	0.3831
P2_Flex/Ext_Ang_Vel [deg/sec]	231.83±111.52	292.66±84.37	0.1032
Peak_Flex_Ang_Vel [deg/sec]	106.52±44.34	147.33±48.46	0.0115*
Peak_Ext_Ang_Vel [deg/sec]	146.65±81.12	165.62±50.41	0.4482
Initial_Flex_Ang_Acc [deg/sec^2]	3.32±4.79	2.86±1.64	0.7279
Pre_Seat-off_Flex_Ang_Dece [deg/sec^2]	-4.69±4.20	-4.99±3.27	0.8313
Post_Seat-off_Ext_Ang_Acc [deg/sec^2]	-5.35±4.85	6.88±4.33	0.3714
t1_ Peak_Flex [sec]	1.27±1.00	0.73±0.33	0.0556
t2_Seat-off [sec]	1.24±0.47	0.73±0.20	0.0005*

t3_ Peak_Ext [sec]	1.21±0.46	0.76±0.30	0.0032*
t4_Swing_TO [sec]	1.91±1.05	1.02±0.33	0.0041*
t5_Swing_HS [sec]	2.37±±1.07	1.49±0.27	0.0045*
t6_Stance_TO [sec]	2.43±1.14	1.52±0.30	0.0052*
t7_Stance_HS [sec]	2.94±1.15	1.99±0.31	0.0042*
t8_Initital_Gait_Cycle [sec]	1.33±0.15	0.96±0.11	<0.0001*
t9_TotalSingleStance [sec]	1.26±0.08	0.94±0.12	<0.0001*
t10_GI_PartialDoubleSupport [sec]	0.37±0.08	0.025±0.047	<0.0001*
t11_ Between Peak Flex./Ext. Momentums [sec]	1.02±0.91	0.48±0.17	0.0312*
t12_PeakFlexion to Seat-off [sec]	0.66±0.50	0.26±0.12	0.0045*
t13_Seat Off to Peak Extension [sec]	0.66±0.44	0.22±0.12	0.0009*
t14_Time_to_STW_Completion [sec]	2.94±1.15	1.99±0.31	0.0042*

3.4.4 Postural stability (PS) parameters between fallers and non-fallers

Table 3-6 summarizes the results of the PS parameters between fallers and non-fallers. No significant differences were found in the results.

Table 3-6: Results of the PS parameters between fallers and non-fallers.

Postural Stability parameters	Fallers	Non-fallers	p-value
Open Eyes Sway Velocity (m/s)	0.0133±0.0029	0.0127±0.0022	0.2032
Open Eyes Mean Radius (m)	0.0038±0.0010	0.0029±0.0010	0.1017
Closed Eyes Sway Velocity (m/s)	0.0172±0.0045	0.0153±0.0028	0.0893
Closed Eyes Mean Radius (m)	0.0045±0.0031	0.0033±0.0011	0.1284

3.5 Discussion

The purpose of this study was to investigate the relationship between gait and postural parameters and fall risk among older adults. First, the gait parameters were investigated between fallers and non-fallers. It was determined that two parameters: *gait cycle time* and *double support time*, were significantly different between fallers and non-fallers. Fallers had longer gait cycle times, which suggests that fallers spend more time with their feet in contact with the ground in absolute time -- reflected by increased double support times. Previous studies demonstrated similar results. Wu and Lockhart [186] reported that fallers have longer gait cycle times (1.16±0.14(s)) compared to non-fallers (0.92±0.27(s)). Additionally, they reported that fallers have a longer double support time (0.28±0.12(s)) compared to non-fallers (0.23±0.11(s)), which are consistent with our findings. One explanation for this difference might be that non-fallers have more confidence or less fear of falling compared to fallers, which also may affect the gait patterns. Fallers may have increased second double support time to reduce perturbations to balance during walking.

No significant differences were found on the other gait parameters (e.g. gait speed, step length…etc.). The results are in agreement with the study of Toulotte et al. [187] which reported no significant difference between healthy elderly fallers and non-fallers walking freely under single-task conditions. Similar results also were found by Gehlsen and Whaley [188]; they found no differences between fallers and non-fallers in numerous temporal gait parameters. Pijnappels et al. [189] also reported that walking speed did not differ between fallers and non-fallers. However, some studies reported contrasting results, in which they demonstrated that fallers have shorter stride and step lengths, and slower walking speeds, compared to non-fallers [190-194]. For example, Imms and Edholm [193] found that fallers have reduced walking speeds and shorter step lengths. Wolfson et al. [194] reported similar results in nursing-home residents.

For the sit-to-stand (STS) postural parameters, five parameters were significantly different between fallers and non-fallers (*Peak_Flex_Ang_Vel, Late_Ext_Ang_Acc, t1_Peak_Flex*, *t4_CompleteSTS,* and *t8_ Peak_Ext_Ang_Momentum to Termination*).

Angular velocity and acceleration values, over the total assessment were lower in fallers, indicating less smooth movement in this category. One explanation for this finding may be reduced quadricep strength and core muscle strength in fallers.

The results are in accordance with the study of Doheny et al. [195], which indicated that fallers take a significantly longer time to complete an STS task compared to non-fallers. Similarly, Najafi et al. [115] reported increased mean postural transition duration for fallers.

Additionally, fallers needed a significantly longer time to initiate movement (*t1_Peak_Flex*) compared to non-fallers, suggesting that fallers struggle with the flexion phase of postural transition compared to non-fallers. Likewise, fallers delineated longer stability times (*t8_ Peak_Ext_Ang_Momentum to Termination*), which indicate that they require more time to maintain stability following STS postural transitions. However, previous studies have demonstrated the value of determining the time taken to complete a five-time-STS to identify fall risk [180]; with a time greater than 15 seconds, as reported by Buatois et al., indicating increased fall risk [196]. The fallers examined in the present study took longer to complete the five-time-STS than the non-fallers. Thirty participants were examined in the community dwelling environment, which may not be sufficiently large to replicate the observations of Buatois et al., who examined 2735 participants in a clinical environment [196].

For the sit-to-walk (STW) test, the findings demonstrate that most parameters and transition events were significantly different between fallers and non-fallers. Because sit-to-walk is a more complex task compared to the sit-to-stand task, the identification of specific components during the transition from sitting to walking among the elderly may help identify mobility problems in various phases of the transition. However, the acquisition of STW information requires three IMUs: one on the sternum, and the other two on right and left shank.

For the postural stability (PS) test, sway average velocity and mean radius recordings -- in the open eyes and closed eyes conditions -- were utilized to distinguish fallers and non-fallers. There were no significant differences between fallers and non-fallers. Similar to the study of O'Sullivan et al., they found it was difficult to identify differences between fallers and non-fallers on a firm surface, since standing on a firm surface produces less sway response than standing on a foam [157]. They also found there was a significant difference in postural stability parameters between fallers and non-fallers when the participants were tested while standing on a mat. This is in agreement with Kamen and Cho's studies that determined the ability of IMUs to discern tasks of increasing difficulty [191, 197]. In future investigations, standing on a foam should be used for postural stability testing, to better distinguish fallers and non-fallers.

In summary, there were differences in gait and postural parameters in fallers and non-fallers; most of the tasks required three IMUs to achieve ample information. The STW test is able to offer the most gait and postural parameters to distinguish fallers and non-fallers, but it requires three IMUs (located on the sternum, left and right shank). Because the STW task includes both walking and STS phases, it could provide more robust information when comparing walking or an STS task only.

As we are seeking an approach to utilize only one IMU to identify fallers and non-fallers, we turn to machine learning techniques to classify fallers and non-fallers, based on appropriate gait and postural features which can be obtained from only one sensor located on the sternum.

Chapter 4 STUDY II: SUPPORT VECTOR MACHINE BASED FALLERS AND NON-FALLERS CLASSIFICATION

4.1 Objective

The objective of this study is to develop and evaluate machine learning algorithm, specifically support vector machines, for classifying fallers and non-fallers with IMUs. It was hypothesized that only one IMU located at sternum is enough to classify fallers and non-fallers by the SVM classifier.

4.2 Methods

4.2.1 Subjects, apparatus and experimental protocols

All subjects and apparatus are the same as described for Study I (see Chapter 3). However, in this study, only the task of normal walking was utilized to classify fallers and non-fallers. Additionally, only one IMU located at sternum was used in this study.

4.2.2 Data analysis

Based on the findings of previous studies [198, 199], we used a 67%/33% split for training and testing sets. Thus, twenty sets of data (10 fallers and 10 non-fallers) were used for training, and ten sets (5 fallers and 5 non-fallers) of data were used for testing. First, the original IMU data was scaled for conveniently solving large datasets, and then Principle Component Analysis (PCA) [200, 201] was employed to decrease the data dimensions. Subsequently, the SVM algorithm was utilized to classify fallers and non-fallers (Figure 4-1).

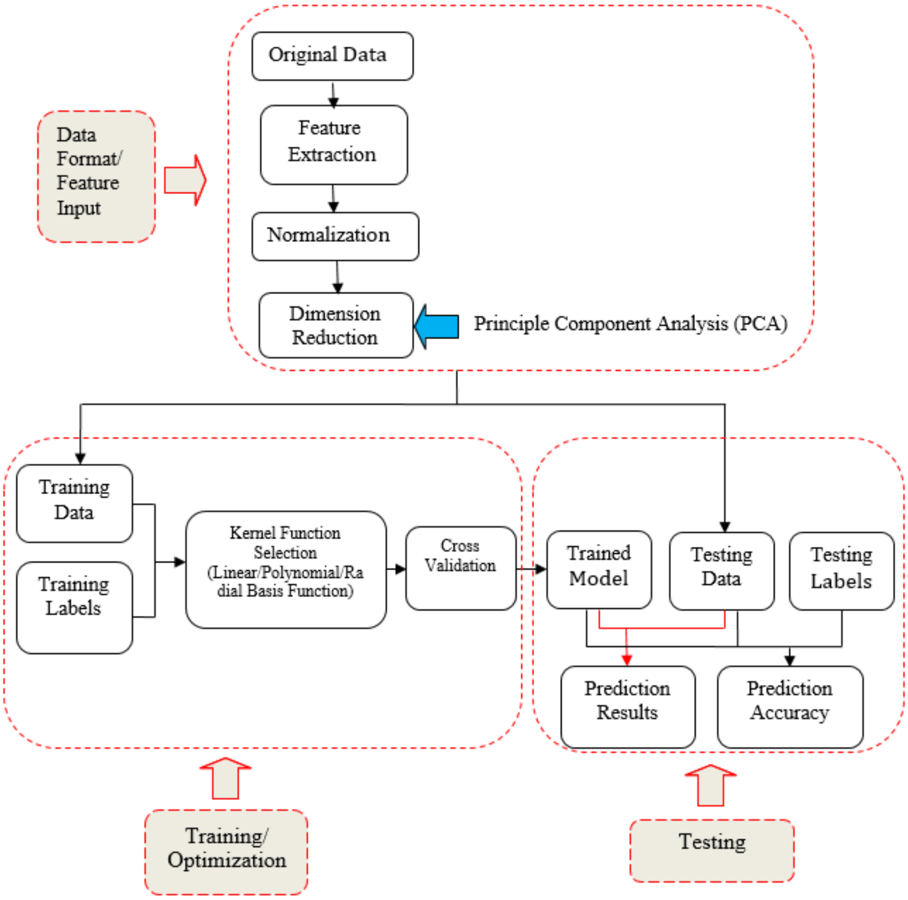

Figure 4-1: Data analysis procedure.

<u>Input data to the SVM classifier</u>: The original data was collected by an IMU at the sternum. The IMU provided three directional accelerations and angular velocities. The format of the original data was a matrix with 6 columns, representing 6-channel signals from tri-axial accelerometers and gyroscopes. The task of normal walking was used as the SVM classifier input. IMU signals from the sternum were truncated into 2-second data segments to ensure the completion of one gait cycle [170].

<u>Training and testing sets</u>: For the classification, both training and testing data sets consisted of fallers and non-fallers data. Totally 30 datasets (30 participants: 15 fallers and 15 non-fallers) were selected for classification of fallers and non-fallers. All of the datasets were then split into training and testing set: 20 (10 fallers and 10 non-fallers) training set and 10 (5 fallers and 5 non-fallers) testing set. Since training set was kept around 70% of the total number of sets whereas the remaining around 30% was kept for testing [198, 199].

Feature extraction methods: Two different feature extraction methods were used to select features. One method adopted general feature information from both temporal and frequency domains; and the other one utilized kinematic features as input.

General features - The general features were chosen to include all possible spatial and temporal information from the walking signals. Based on the criterion of minimizing computational complexity and maximizing the class discrimination, several key features have been previously proposed for SVM classification [202]. All features in this study have been extracted from raw signals, and they are displayed as below:

Mean Absolute Value - The mean absolute value of the original signal, $\bar{x}$, in order to estimate signal information in time domain:

$$\bar{x} = \frac{1}{N} \sum_{k=1}^{N} |x_k| \qquad (4.1),$$

where x_k is the k_{th} sampled point and N represents the total sampled number over the entire signal.

Zero Crossings – Zero crossing is defined as the number of times the waveform crosses zero, in order to reflect signal information in frequency domain.

Slope Sign Changes – It is the number of times the slope of the waveform changes sign, which reflects frequency content of the signal.

Length of Waveform – It represents the cumulative curve length over the entire signal, in order to provide information about the waveform complexity.

Dominant Frequency – Signals were filtered using Butterworth low-pass filter of 4th order with cut-off frequency of 6 Hz. Fast Fourier Transformation (FFT) was carried out on the filtered signal and the dominant frequency was defined as the frequency with the highest magnitude.

Other general features included mean, standard deviation, maximum, minimum, skewness, kurtosis, and energy of original signal segments. All of these features would give a measure of waveform amplitude, frequency, and duration within a single parameter. Table 4-1 elaborates general features used in this study.

Table 4-1: General features used for SVM input.

General features: Accelerometer (A_x, A_y, A_z) and gyroscope (G_x, G_y, G_z) signals in all 3 directions of original data
• Mean • Standard deviation • Maximum • Minimum • Mean absolute value: $\bar{x} = \frac{1}{N}\sum_{k=1}^{N}\lvert x_k\rvert$ • Skewness • Kurtosis • Energy • Number of slope sign changes

- Number of zero crossings
- Length of waveform
- Dominant frequency using low-pass filter and FFT

Selected Features – In total, 11 kinematic features were selected from the resultant walking acceleration and jerk. Resultant acceleration was calculated from the raw accelerometer data:

$$R = \sqrt{A_x^2 + A_y^2 + A_z^2} \quad (4.2),$$

where A_x, A_y, A_z are accelerations sensed by triaxial accelerometer situated on sternum. Jerk is computed as a derivative of resultant acceleration. Resultant acceleration and jerk of the trunk segment and their derived features, such as mean, maximum, minimum, range, energy and dominant frequency while walking are very important as they provide complete kinematics of the trunk. Skewness of resultant accelerations and jerk provides information of the temporal shift of peak accelerations and jerk from the walking signals. Jerk cost, as described by the area under squared jerk curve is an important measure to estimate the energy economy of walking.

$$JC = \int_0^T |\frac{d^3r}{dt^3}|^2 dt \quad (4.3).$$

During walking, minimizing jerk and minimizing energy are believed to be complementary performance criteria [203]. Table 4-2 summarizes kinematic features used in this study.

Table 4-2: Kinematic features used for SVM input.

Kinematic features	Resultant acceleration ($R = \sqrt{A_x^2 + A_y^2 + A_z^2}$) Resultant Jerk ($J = \frac{dR}{dt}$)

Resultant acceleration features	• Skewness (temporal shift) • Energy • Dominant frequency • Maximum acceleration • Minimum acceleration • Range of acceleration
Resultant jerk features	• Mean jerk • Absolute maximum jerk • Absolute minimum jerk • Range of jerk produced abs (max-min) • Jerk cost $JC = \int_0^T \lvert \frac{d^3r}{dt^3} \rvert^2 dt$

Input data processing: Preprocessing of features is usually required before using the SVM classifier to maximize the classification accuracy. The input features derived from signals were normalized, and the dimension of the feature space was reduced using principal component analysis.

a) *Normalizing input data*: All of the features values were normalized by combining training and testing feature space and dividing all of them by the maximum value of that particular feature. In this type of scaling the input data was kept in the range of 0 to 1, and 1 represented the maximum value of the feature.

b) *Dimension reduction of feature space*: Principle Component Analysis (PCA) [204] was employed to decrease the dimensions. The objective of PCA is to perform dimensionality reduction while preserving as much of the randomness in the high-dimensional space as possible.

c) *Kernel schemes*: A kernel is a function that transforms the input data to a high-dimensional space where classification is possible. Kernel functions can be linear or nonlinear. Kernel selection plays an important role in acquiring high accuracy from SVM classification. An appropriate kernel may minimize generalization error, and increase classification accuracy. The linear kernel function is the simplest kernel function and works well when there are many features in the training data. Radial Basis Function (RBF) kernel is usually the first reasonable choice as it can nonlinearly map data into higher dimensional space. Polynomial kernels are non-stationary kernels and are well suited for normalized training data.

d) *Cross-validation*: Cross-validation is a standard technique usually adopted for adjusting hyperplane parameters to improve the quality of its estimates in SVM model. A five-fold cross-validation scheme was adopted to evaluate the generalizability of the SVM classifier [205, 206]. In cross-validation procedure, the training data set is uniformly divided into five subsets with one used for testing and the other four used for training and constructing the SVM decision surface. This process is continued until all subsets are used as the testing sample.

e) *Performance assessment of SVM classifier*: All SVM models were trained over the range of cost parameter, C (2^{-10} to 2^{10}) using linear, polynomial and radial basis function kernel. The cost parameter C controls the tradeoff between training error and margins. The criterions used to assess the classification performance of SVM classifier were:

$$Accuracy = \frac{TP+TN}{TP+FP+TN+FN} \times 100\% \qquad (4.4),$$

$$Sensitivity = \frac{TP}{TP+FN} \times 100\% \qquad (4.5),$$

$$Specificity = \frac{TN}{TN+FP} \times 100\% \qquad (4.6),$$

where TP represents the number of true positives, TN is the number of true negatives, FP indicates the number of false positives, and FN represents the number of false negatives. While accuracy indicates overall detection accuracy; sensitivity is defined as the ability of the SVM classifier to accurately classify fallers and non-fallers; and specificity would indicate the SVM classifier's ability to avoid false detection.

Furthermore, Receiver Operating Characteristic (ROC) curve was also used to evaluate SVM classifier's performance. ROC analysis is generally utilized to select optimal models and to quantify the accuracy of diagnostic tests. Besides, the Area under the ROC Curve (AUC), which is a representation of the classification performance, was utilized to assess the effectiveness of SVM classifier. Further, tests were also conducted to evaluate performance of the SVM classifier in three different kernel functions: linear, polynomial, and radial basis function (RBF) kernels.

4.3 Results

The machine learning classification results demonstrated high classification rates across all three types of kernel (i.e., linear, polynomial and RBF kernel) for both types of feature selection approaches. We found that linear (accuracy 90%) and polynomial (accuracy 90%) kernels performed equally well in fallers and non-fallers classifications (Table 4-3). And polynomial kernel had the lowest classification accuracy (about 80%) amongst all three different types of kernels.

Table 4-3: Fallers and non-fallers classification using IMU derived features. Accuracy, sensitivity, specificity and AUC (area under the Receiver operating curve) are tabulated for three kinds of feature selections methods and three kernels.

Fallers and non-fallers classification				
		Linear	Polynomial	RBF
General Features	Accuracy	0.90	0.90	0.80
	Sensitivity	0.90	0.90	0.80
	Specificity	0.80	0.80	0.90
	AUC	0.90	0.90	0.90
Kinematic Features	Accuracy	0.90	0.90	1.00
	Sensitivity	0.90	0.80	1.00
	Specificity	0.96	0.90	1.00
	AUC	0.96	0.90	1.00

Computation time for linear kernel was 90.75 seconds, polynomial kernel required 33.16 seconds and RBF kernel required 39.58 seconds for the classification. The fallers and non-fallers classification results from three different kernels are shown in Figure 4-2. Linear kernel defines a linear boundary to achieve classification (Figure 4-2 a). Polynomial kernel utilizes polynomials of the original input data to classify fallers and non-fallers (Figure 4-2 b). It belongs to nonlinear classification, and has more complexity and better performance when compared to linear kernel. Radial basis function (RBF) kernel is the most popular kernel function, and the two curves running through support vectors are the nonlinear counterparts of the convex hulls (Figure 4-2 c).

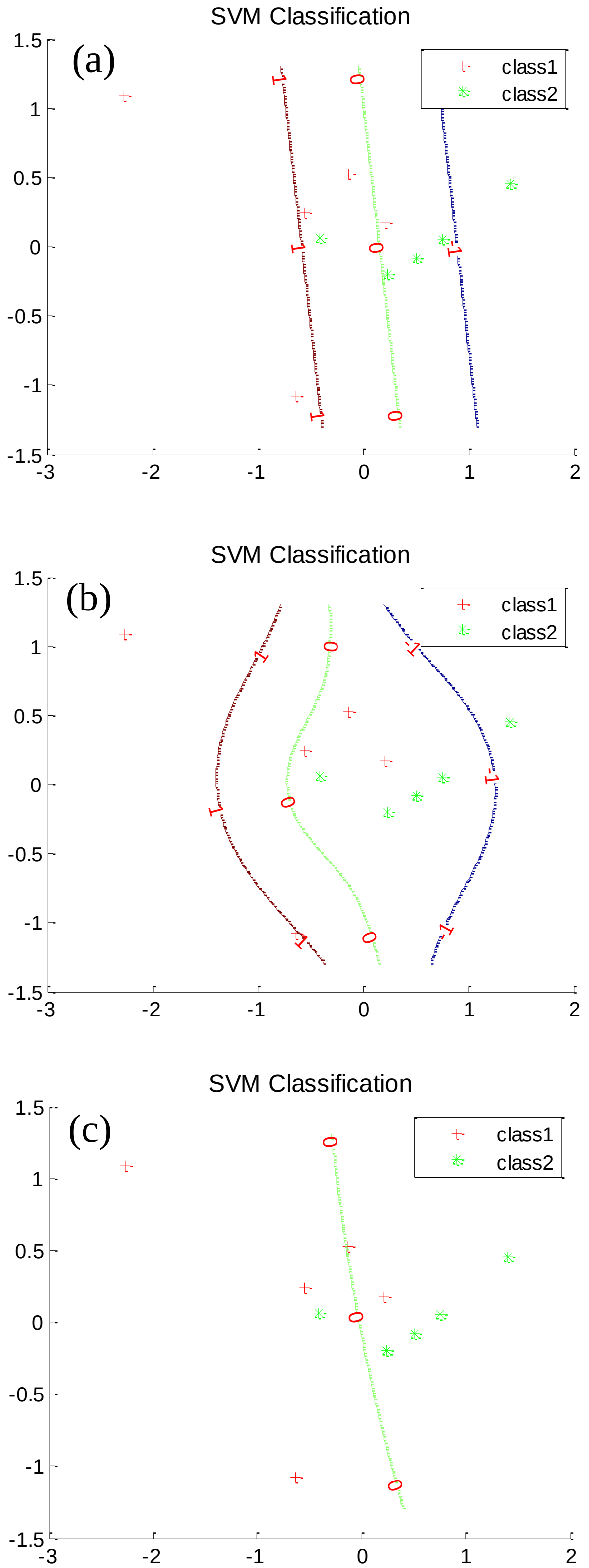

Figure 4-2: Fallers and non-fallers classification results via three different kernels: (a) linear kernel; (b) polynomial kernel, and (c) radial basis function kernel.

4.4 Discussion

In this study, we explored the classification potential of SVM in recognition of gait patterns utilizing only one inertial measurement unit (IMU) associated with fallers and non-fallers. In the previous chapter, the results indicated that there were differences between fallers and non-fallers for some of the gait parameters. In this study, the results showed that, although these changes of gait parameters are subtle, they can provide helpful information for the SVM classifier to classify fallers and non-fallers.

Gait and postural adaptations associated with fall risk, as described in Chapter 3, may influence the walking patterns and these changes associated with fall risks may be utilized to classify fallers and non-fallers. Assuming, walker's body mass to be a point mass, and a rigid strut connecting it to the point of ground contact. This point mass reaches the highest point at the middle of the stance phase [207-209]. The trajectory of whole body center-of-mass (COM) follows a sinusoidal path along vertical direction [207-210], which may be related to fall risk. Similarly in walking, IMU located at the sternum allowed the measurement of mechanical work done during walking (i.e., inducement of fall risk and its associated relationship to economy during walking as assessed by the jerk cost). Energy is defined as the external work done by muscles to maintain locomotion and is highly correlated with vertical displacement of COM. An approach to minimize vertical movements of the COM (at sternum level) was detailed by Inman and his colleagues [211], in which they identified several mechanisms involved in flattening the trajectory of the COM [211, 212], including sagittal plane knee flexion and extension during stance phase. However, with fall risks, flattening of the trajectory of the COM may not be efficient due to the kinematics of lower extremity joints. For example, Kellis and Liassou found that fallers decreased ankle dorsiflexion [213].

Previous researchers have adopted various gait feature extraction methods for SVM classification. Begg and coworkers differentiated elderly and young gait patterns using general features on minimum foot clearance data [29]. In another study, they selected kinetic and kinematic gait features for classification [31]. Whereas Eskoifer et al. adopted concatenated waveforms from infrared markers to classify young and elderly gait [72]. Results of our investigation (Table 4-3) indicate that feature extraction methods influenced classification accuracy. In fallers and non-fallers classification, both kinds of input, general feature and selected feature input performed well.

Three different types of kernels were employed in SVM classifier: linear, polynomial, and RBF. Both linear and RBF kernels performed well in general feature of falls and non-falls classification, which complied with Lee and Grimson's report [214], showing that linear kernel performs better than polynomial kernel in SVM gait recognition. However, for selected feature input, RBF performed better than the other two kernels. Considering the computational cost, RBF and polynomial kernels need less time compared to linear kernel in the same conditions. As such, RBF kernel is the most promising kernel function in the fallers and non-fallers classification schemes, and it may also provide better applicability to real time system implementation.

In summary, only one IMU located in sternum is able to classify fallers and non-fallers, through the information from normal walking activity. In Chapter 3, we found that there are significant differences in gait and postural parameters between fallers and non-fallers. And this study validates the hypothesis that the SVM classifier is able to classify fallers and non-fallers only using one IMU located at the sternum by utilizing the subtle changes of gait parameters.

Chapter 5 STUDY III: ROBUSTNESS OF SVM APPLIED IN CLASSIFICATION OF FALLERS AND NON-FALLERS

5.1 Objective

This study investigates the robustness of SVM algorithms associated with classification of fallers and non-fallers. To evaluate the robustness of the SVM algorithm, the effects of two parameters involved in SVM algorithm - the soft margin constant C and the kernel function parameter γ are investigated. Furthermore, white noise is added into the signals, and the effects of these two parameters on the classification accuracy are further discussed. It was hypothesized that the SVM classifier is robust enough to classify fallers and non-fallers in noisy environment, by adjusting the parameters accordingly.

5.2 Theoretical Analysis

The SVM algorithm has two important parameters called hyper-parameters: soft margin constant C, and the other parameter γ reflecting the kernel function. In this study, Gaussian kernel was applied to the SVM classifier; correspondingly, γ refers to the width of a Gaussian kernel.

For the parameter C, it reflects the tradeoff between the margin and error. When C value is large, margin error is small; however, the margin becomes narrow as a penalty. When C is small, those points close to the boundary become margin error; but the hyperplane's orientation would change, providing a much larger margin for the rest of the data.

As for the other parameter γ, the expression the Gaussian kernel is:

$$k(x, x') = exp(-\gamma\|x - x'\|^2) \qquad (5.1).$$

The Gaussian basis function with center $\vec{x_i}$ and variance σ_i^2 can be constructed as:

$$\mathcal{G}(\vec{x}) = \frac{1}{(2\pi)^{d/2}\sigma_i^d} exp\left(-\frac{\|\vec{x}-\vec{x_i}\|^2}{2\sigma_i^2}\right) \qquad (5.2),$$

where d is the dimensional number of Gaussian RBF.

If we construct an SVM Gaussian RBF classifier as:

$$\sum_{i=1}^{l} y_i\, \alpha_i \cdot exp\left(-\frac{\|x-\vec{x_i}\|^2}{c}\right) + b) \qquad (5.3),$$

where $y_i = f_{w,b}(x_i)$; w is known as the weight vector, b is a bias term, α_i is Lagrangian multipliers, c is the constant. To optimally choose the centers of $\vec{x_i}$, the centers points which are critical to the classification task would be selected. In other words, if the unknown sample x goes away from the known sample centers of $\vec{\mathrm{x_i}}$, there will be a decay and, we can use this kernel to assign weights (i.e., decision weights). The SVM algorithm implements this idea. The algorithm automatically computes the number and location of the above centers, and provides weights w_i, and the bias b by means of the Gaussian kernel function. Therefore, in the RBF kernel case, SVM classifier utilizes the Gaussian kernel function to select centers, weights and apply threshold in order to minimize an upper bound on the expected test error. The advantage of the RBF approach is that it utilizes local approximators to map input to output, so that the system computes fast and requires fewer training samples.

In essence, γ reflects the flexibility of the decision boundary. When γ is small, it would generate a smooth decision boundary, nearly linear. When γ is large, it would generate a great curvature of the decision boundary. When γ is too large, it will cause overfitting, as shown in Figure 5-1 (d). Figure 5-1 and Figure 5-2 illustrate the effect of these two parameters, γ and C, on the decision boundary.

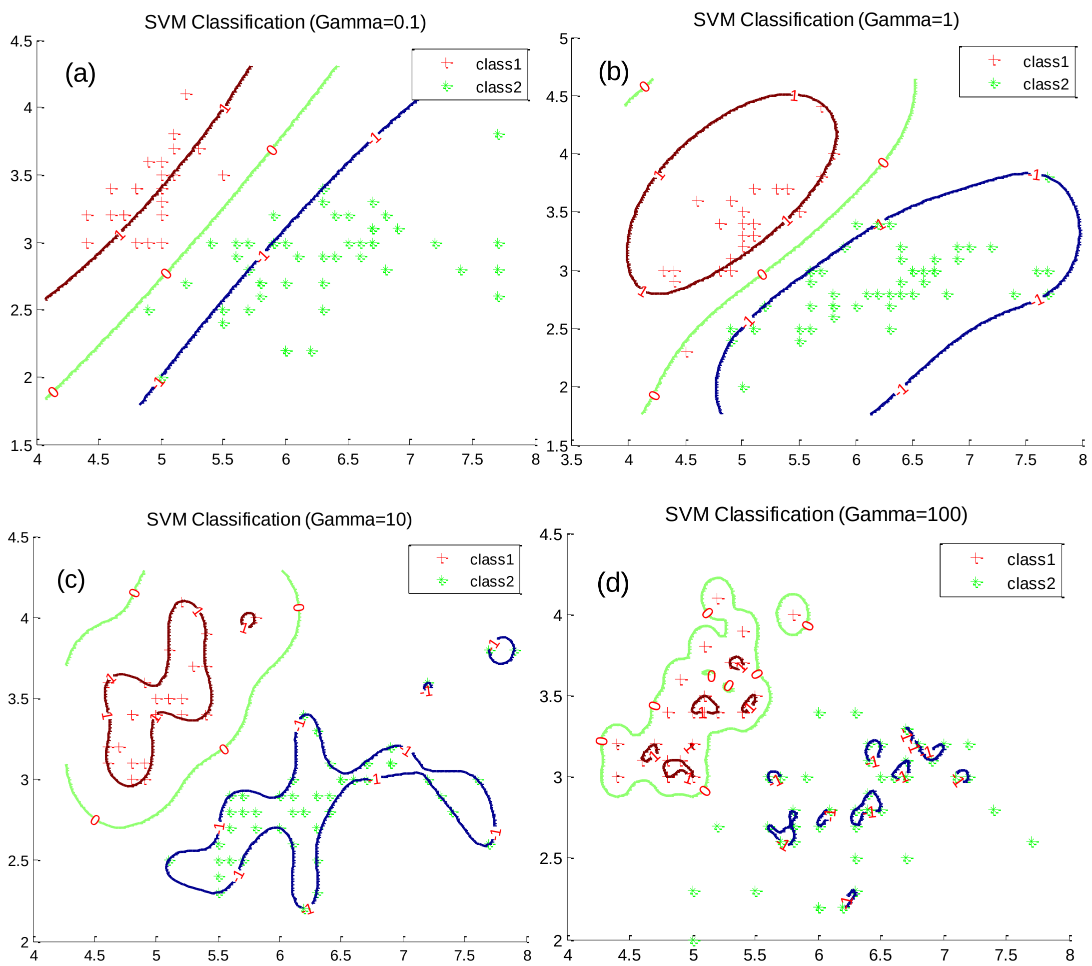

Figure 5-1: The effect of the parameter γ, on the decision boundary. (a) When $\gamma = 0.1$, the decision boundary is nearly linear. (b) When $\gamma = 1$ the curvature of decision boundary increases. (c) When $\gamma = 10$, the curvature of decision boundary continues increasing, and causes a little overfitting. (d) When $\gamma = 100$, overfitting becomes serious in the classification. (Gamma is used to represent γ in the figure.)

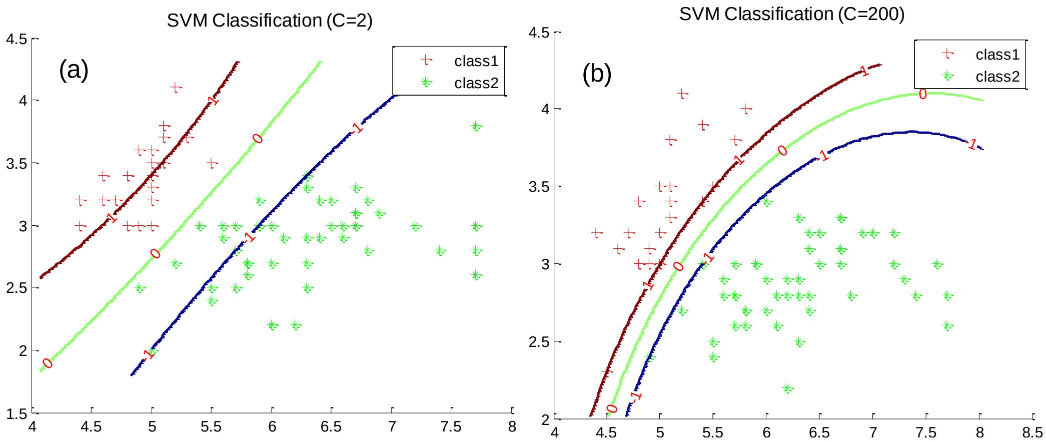

Figure 5-2: The effect of the soft-margin constant, C, on the decision boundary. (a) When C = 2, it increases the margin and ignores the data points close to the decision boundary. (b) When C = 200, it decreases the margin and margin error.

To find the optimal values for the two parameters, the cross-validation and grid-search were utilized. In v-fold cross-validation, v means the number of input data splits. The training data is divided into v subsets equally. Any $v-1$ subsets are selected for training the model, and then the remaining subset is predicted based on the constructed model. The same procedure is rotated in all the subsets while keeping the equal chance being predicted for each subset. Therefore, each subset of the input data would be predicted once so the cross-validation accuracy is the percentage of data which are correctly classified.

An approach combining grid-search method and cross-validation was proposed for searching the optimal C and γ. Different pairs of $(C,\ \gamma)$ values were tried for predicting data, and only the best cross-validation accuracy was selected. There were only two parameters for search, thus it did not require too much of computational time, satisfying the demand of SVM classification.

Here is a case of the SVM classification result comparison between the random parameters and optimal parameters. Firstly 60 sets of data were split into training data and test data evenly, and then LibSVM [169] with random SVM parameters was used to obtain the classification accuracy of 60%. Next, the grid-search and cross validation methods were applied to find the optimal C and γ values (effects of selecting the optimal C and γ value as compared to selecting the parameters in random are illustrated in Figure 5-3).

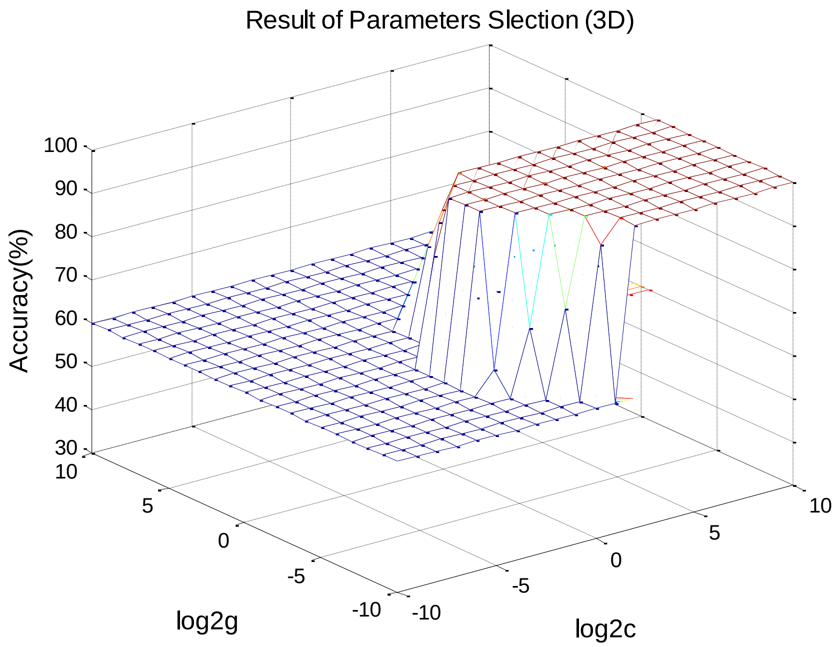

Figure 5-3: Searching the optimal C and γ value in three-dimension coordinates.

The validation accuracy increases from 60% to 100%. However, there were several solution-sets of C and γ satisfying the 100% accuracy, and here, the minimum C value was chosen as the optimal C, and the corresponding γ was chosen as the optimal value since high C value can improve the validation accuracy, however, it would also cause over-learning, and would affect the final classification prediction accuracy. Therefore, the optimal C was chosen as 0.2500 and γ was chosen as 0.0313 in this case.

5.3 Experimental Analysis

As the assessment of fall risk is linked to understanding the unwanted signals (i.e., noises) as well as wanted signals, it is important to understand the capability of the SVM classifier to effectively address noisy data. Therefore, the change of the parameters involved in the SVM algorithm along with the added white noise was investigated.

To systematically evaluate the robustness of the SVM algorithm, the white noise was added into the normal walking data with different levels of signal-to-noise ratio (SNR). The SNR measure in the study was defined as:

$$SNR = 10\, log_{10}(p_1/p_2) \qquad (5.4),$$

where p_1 is the power of the normal walking data, and p_2 is the power of the noise.

The white noise was added into the normal walking data with SNR from 10 to 0.2. And the same classification approaches as Chapter 4 were applied to the data sets. The results are shown in Table 5-1. Additionally, Figure 5-4 and Figure 5-5 illustrate the results from Table 5-1.

Table 5-1: Classification accuracies of fallers and non-fallers associated with SNR.

	SNR	10	9	8	7	6	5	4	3	2	1	0.8	0.5	0.2
General Features	Linear	0.9	0.9	0.9	0.9	0.9	0.9	0.8	0.8	0.7	0.7	0.5	0.4	0.4
	Polynomial	0.9	0.9	0.9	0.9	0.9	0.9	0.9	0.8	0.8	0.8	0.6	0.6	0.6
	RBF	0.8	0.8	0.8	0.8	0.8	0.8	0.8	0.8	0.8	0.8	0.7	0.6	0.6
Kinematic Features	Linear	0.9	0.9	0.9	0.9	0.9	0.9	0.8	0.7	0.7	0.6	0.5	0.5	0.5
	Polynomial	0.9	0.9	0.9	0.9	0.9	0.9	0.9	0.8	0.8	0.6	0.6	0.6	0.6
	RBF	1	1	1	1	1	1	1	1	1	0.9	0.8	0.8	0.8

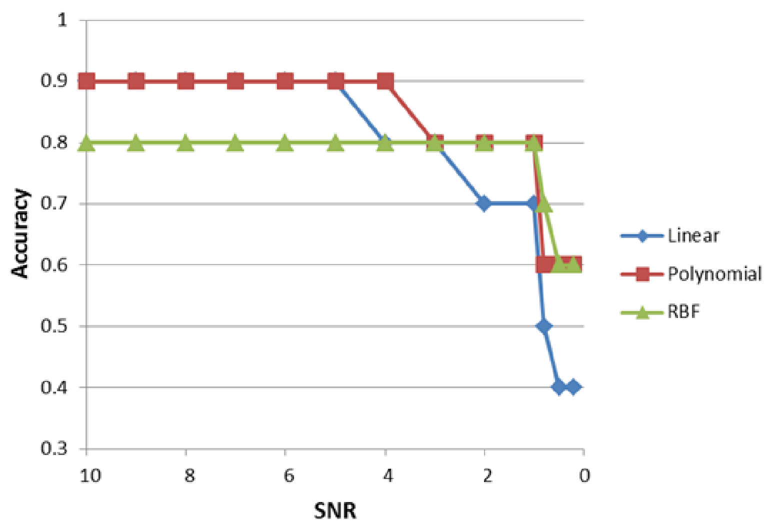

Figure 5-4: Classification accuracies of fallers and non-fallers associated with SNR by general features.

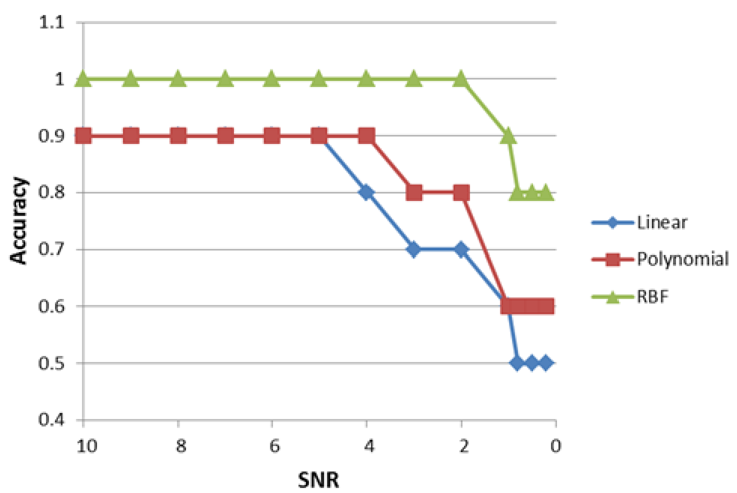

Figure 5-5: Classification accuracies of fallers and non-fallers associated with SNR by kinematic features.

5.4 Discussion

Information presented in this chapter focuses on the variation of the optimal parameters involved in SVM algorithm: C and γ; as well as the applicability of SVM as a machine classifier to distinguish fallers and non-faller in the noisy environment. As the performance of different classifiers can be assessed by modulating the noise conditions [215, 216], this study utilized the white-noise to create a noisy environment in order to evaluate the classification capability of SVM classifier. Considering the large human movement variation, the range of SNR (0-10 dB) was chosen largely enough for the robustness. For the normal walking data, both training and test sets were contaminated by white-noise; however, the SVM classifier still can stably maintain high classification accuracy by optimizing the two parameters C and γ. Previous studies have reported that C and γ could modulate themselves for noisy data [217], which is accordant to our analytic results.

In addition, the RBF kernel showed more robustness comparing to the linear and polynomial kernel, which is consistent with previous studies [218]. In summary, the parameters in the SVM classifier is robust enough to classify fallers and non-fallers in noisy environments.

Chapter 6 SUMMARY AND FUTURE WORK

6.1 Major Findings

First, this study investigated the relationship of gait and postural parameters between fallers and non-fallers from IMU data, in order to distinguish these two groups. Statistical analysis suggests that there are some significant differences between fallers and non-fallers; however, three IMUs – one located at the sternum and two others located at each shank – are needed to achieve this finding.

Then the machine learning method - support vector machine (SVM) classifier – was employed to classify fallers and non-fallers. Different gait feature extraction methods for SVM classification were investigated and compared for classifying fallers and non-fallers. Additionally, three different types of kernels: linear, polynomial, and RBF were compared with the classification results. Both linear and RBF kernels performed well in general feature of fall and non-fall classifications; and for selected feature input, RBF performed better than the other two kernels. Considering the computational cost, RBF and polynomial kernels need less time compared to the linear kernel in the same conditions. The results of the study show that only one IMU located on the sternum is able to classify fallers and non-fallers by SVM classifier.

To further expand the applications of the SVM classifier, the robustness of the SVM classier was investigated. Two parameters that affect the performance of the SVM algorithm - the soft margin constant C, and the other parameter reflecting the kernel function γ - have been systematically investigated. From the results, we can conclude that the SVM classifier has the power to classify fallers and non-fallers in a noisy environment. And this study demonstrates the potential of the SVM classifier to classify fallers and non-fallers by utilizing only one IMU located at the sternum.

Several health applications associated with this study could be implemented. Along with providing fundamental findings on the effects of gait and postural parameters, factors thought to be responsible for increased risk of falls have been thoroughly evaluated. Additionally, we have successfully implemented the classification of fallers and non-fallers by using only one IMU located on the sternum. Differences between fallers and non-fallers groups will be helpful to explain the higher rate of falls in the older adults with gait adaptations. The use of IMUs provides a platform of non-intrusive, continuous, remote mobility analysis and fall risk assessment for the elderly adults, due to the less burden of wearable sensors. It can be applied in health care facilities in the future, such as nursing houses and assisted living facilities, etc.

6.2 Limitations and Future Work

Several limitations existed in this study. First, the sample size for the study was not that large. The power was calculated as 0.8 by using the *double support time* parameter ($\text{difference of mean values } = 0.09;\ \text{pooled standard deviation} = 0.8631;$ $\alpha = 0.05$). Additionally, the diversity of sample should be considered, in order to develop a robust fall risk assessment model that can be used in the community settings. Specifically, more participants are needed in the future with wide variations in age, health condition, and other demographic conditions.

Second, only one location (sternum) of the IMU was investigated in this study. Other sensor locations, such as the waist, thigh, and shank were not considered. Although one IMU located at the sternum is good enough to classify fallers and non-fallers with walking data, more features and factors should be considered in the future.

Fall risk assessment is only the first step of our research. In the future, a prediction model for fall prone individuals should be investigated. The reliability models based solely on event records, such as fall accident events of history records, have been reasonably well developed for predicting fall prone individuals. However, these approaches only provide general or average estimates for the entire population. Besides, fall behavior is a function of changes in work schedule, operating environment and other parameters. In the other hand, conditional monitoring data mainly provide information for short-term condition prediction only. Therefore, the prediction of fall prone individuals should be dependent on the combination of general characteristics of the population (such as prior knowledge, historical records, etc.) and short-term condition monitoring. Thus, a systematic prediction strategy which combines the strengths of these two approaches will be developed. The ultimate goal is to predict the fallers and non-fallers based on the established real time monitoring system, as well as prior knowledge. Specifically, machine learning methods, such as machine learning regression methods, have been successfully used for time series prediction and controls. Therefore, it is hypothesized that machine learning approaches can potentially be utilized for fall prediction systems.

References

[1] "Centers for Disease Control and Prevention," April 1-2, 2008.

[2] "World Population Prospects - The 2004 Revision " Department of Economic and Social Affairs - Population Division 2005.

[3] "An older and more diverse nation by midcentury," U.S. Census Bureau2008.

[4] J. Xu, K. D. Kochanek, S. L. Murphy, and B. Tejada-Vera, "Deaths: Final Data for 2007," National Vital Statistics2010.

[5] "Fatal Injury Reports, National and Regional, 1999 - 2010," Centers for Disease Control and Prevention (CDC)2013.

[6] "Nonfatal Injury Reports, 2001 - 2012," 2013.

[7] " Web–based Injury Statistics Query and Reporting System (WISQARS)," Centers for Disease Control and Prevention, National Center for Injury Prevention and Control.2013.

[8] "Ten leading causes of death and injury," Centers for Disease Control and Prevention2011.

[9] J. A. Stevens, P. S. Corso, E. A. Finkelstein, and T. R. Miller, "The costs of fatal and non-fatal falls among older adults," *Injury Prevention,* vol. 12, pp. 290-295, Oct 2006.

[10] (2012). *Costs of Falls Among Older Adults*. Available: http://www.cdc.gov/homeandrecreationalsafety/falls/fallcost.html

[11] T. Lockhart, "Fall accidents among the elderly," in *International encyclopedia of ergonomics and human factors*, W. Karwowski, Ed., 2nd ed. ed Baton Rouge, FL, USA: CRC Press, 2007, pp. 2626 - 2630.

[12] "Centers for Disease Control and Prevention," National Center for Injury Prevention and Control2004.

[13] M. Cesari, F. Landi, S. Torre, G. Onder, F. Lattanzio, and R. Bernabei, "Prevalence and risk factors for falls in an older community-dwelling population," *Journals of Gerontology Series a-Biological Sciences and Medical Sciences,* vol. 57, pp. M722-M726, Nov 2002.

[14] T. E. Lockhart, "An integrated approach towards identifying age-related mechanisms of slip initiated falls," *Journal of Electromyography and Kinesiology,* vol. 18, pp. 205-217, Apr 2008.

[15] T. E. Lockhart, J. L. Smith, and J. C. Woldstad, "Effects of aging on the biomechanics of slips and falls," *Human Factors,* vol. 47, pp. 708-729, Win 2005.

[16] M. H. Woollacott, "Systems contributing to balance disorders in older adults," *Journals of Gerontology Series a-Biological Sciences and Medical Sciences,* vol. 55, pp. M424-M428, Aug 2000.

[17] M. H. Woollacott, A. Shumwaycook, and L. M. Nashner, "Aging and Posture Control - Changes in Sensory Organization and Muscular Coordination," *International Journal of Aging & Human Development,* vol. 23, pp. 97-114, 1986.

[18] G. Gauchard, N. Chau, J. M. Mur, and P. Perrin, "Falls and working individuals:

role of extrinsic and intrinsic factors," *Ergonomics,* vol. 44, pp. 1330-1339, Nov 2001.
[19] N. Lundebjerg, L. Z. Rubenstein, R. A. Kenny, K. J. Koval, F. C. Martin, M. E. Tinetti*, et al.*, "Guideline for the prevention of falls in older persons," *Journal of the American Geriatrics Society,* vol. 49, pp. 664-672, May 2001.
[20] T. Lockhart and J. Liu, "Differentiating fall-prone and healthy adults using local dynamic stability," *Ergonomics,* vol. 51, pp. 1860-1872, 2008.
[21] T. E. Lockhart, J. C. Woldstad, and J. L. Smith, "Effects of age-related gait changes on the biomechanics of slips and falls," *Ergonomics,* vol. 46, pp. 1136-1160, Oct 10 2003.
[22] E. K. Tan, A. Seah, S. J. See, E. Lim, M. C. Wong, and K. K. Koh, "Restless legs syndrome in an Asian population: A study in Singapore," *Mov Disord,* vol. 16, pp. 577-9, May 2001.
[23] W. Karwowski, *International Encyclopedia of Ergonomics and Human Factors*: Taylor & Francis, 2000.
[24] C. L. Vaughan, B. L. Davis, and J. C. O'Connor, *Dynamics of human gait*: Human Kinetics Publishers, 1992.
[25] G. Van B. Cochran, *A primer of orthopaedic biomechanics*: Churchill Livingstone, 1982.
[26] D. A. Winter, "Human balance and posture control during standing and walking," *Gait & Posture,* vol. 3, pp. 193-214, 12// 1995.
[27] "The prevention of falls in later life. A report of the Kellogg International Work Group on the Prevention of Falls by the Elderly," *Dan Med Bull,* vol. 34 Suppl 4, pp. 1-24, Apr 1987.
[28] M. M. Porter, A. A. Vandervoort, and J. Lexell, "Aging of human muscle: structure, function and adaptability," *Scand J Med Sci Sports,* vol. 5, pp. 129-42, Jun 1995.
[29] S. R. Lord, M. W. Rogers, A. Howland, and R. Fitzpatrick, "Lateral stability, sensorimotor function and falls in older people," *Journal of the American Geriatrics Society,* vol. 47, pp. 1077-81, Sep 1999.
[30] J. Lexell, C. C. Taylor, and M. Sjostrom, "What Is the Cause of the Aging Atrophy - Total Number, Size and Proportion of Different Fiber Types Studied in Whole Vastus Lateralis Muscle from 15-Year-Old to 83-Year-Old Men," *Journal of the Neurological Sciences,* vol. 84, pp. 275-294, Apr 1988.
[31] D. A. Skelton, C. A. Greig, J. M. Davies, and A. Young, "Strength, Power and Related Functional Ability of Healthy People Aged 65-89 Years," *Age and Ageing,* vol. 23, pp. 371-377, Sep 1994.
[32] M. C. Do, Y. Breniere, and P. Brenguier, "A biomechanical study of balance recovery during the fall forward," *Journal of Biomechanics,* vol. 15, pp. 933-9, 1982.
[33] M. E. Tinetti and M. Speechley, "Prevention of Falls among the Elderly," *New England Journal of Medicine,* vol. 320, pp. 1055-1059, Apr 20 1989.
[34] J. J. Collins, C. J. De Luca, A. Burrows, and L. A. Lipsitz, "Age-related changes in open-loop and closed-loop postural control mechanisms," *Exp Brain Res,* vol.

104, pp. 480-92, 1995.

[35] G. L. Onambele, M. V. Narici, E. Rejc, and C. N. Maganaris, "Contribution of calf muscle-tendon properties to single-leg stance ability in the absence of visual feedback in relation to ageing," *Gait Posture,* vol. 26, pp. 343-8, Sep 2007.

[36] N. Teasdale, G. E. Stelmach, A. Breunig, and H. J. Meeuwsen, "Age-Differences in Visual Sensory Integration," *Experimental Brain Research,* vol. 85, pp. 691-696, 1991.

[37] J. H. Sheldon, "The effect of age on the control of sway," *Gerontol Clin (Basel),* vol. 5, pp. 129-38, 1963.

[38] S. R. Lord, J. Dayhew, and A. Howland, "Multifocal glasses impair edge-contrast sensitivity and depth perception and increase the risk of falls in older people," *Journal of the American Geriatrics Society,* vol. 50, pp. 1760-1766, Nov 2002.

[39] R. Q. Ivers, R. G. Cumming, P. Mitchell, J. M. Simpson, and A. J. Peduto, "Visual risk factors for hip fracture in older people," *Journal of the American Geriatrics Society,* vol. 51, pp. 356-363, Mar 2003.

[40] W. Chamberlain, "Restriction in upward gaze with advancing age," *Am J Ophthalmol,* vol. 71, pp. 341-6, Jan 1971.

[41] H. B. Menz, S. R. Lord, and R. C. Fitzpatrick, "Age-related differences in walking stability," *Age and Ageing,* vol. 32, pp. 137-142, Mar 2003.

[42] S. K. Schultz, "Principles of neural science, 4th edition.," *American Journal of Psychiatry,* vol. 158, pp. 662-662, Apr 2001.

[43] A. Shumway-Cook and F. B. Horak, "Assessing the influence of sensory interaction of balance. Suggestion from the field," *Physical Therapy,* vol. 66, pp. 1548-50, Oct 1986.

[44] M. S. Redfern, L. Yardley, and A. M. Bronstein, "Visual influences on balance," *J Anxiety Disord,* vol. 15, pp. 81-94, Jan-Apr 2001.

[45] D. R. Kenshalo, Sr., "Somesthetic sensitivity in young and elderly humans," *Journals of Gerontology,* vol. 41, pp. 732-42, Nov 1986.

[46] M. H. Woollacott, "Age-related changes in posture and movement," *Journals of Gerontology,* vol. 48 Spec No, pp. 56-60, Sep 1993.

[47] M. H. Woollacott, A. Shumway-Cook, and L. M. Nashner, "Aging and posture control: changes in sensory organization and muscular coordination," *International Journal of Aging & Human Development,* vol. 23, pp. 97-114, 1986.

[48] A. Y. Benbasat and J. A. Paradiso, "An Inertial Measurement Framework for Gesture Recognition and Applications," presented at the Revised Papers from the International Gesture Workshop on Gesture and Sign Languages in Human-Computer Interaction, 2002.

[49] N. Barbour and G. Schmidt, "Inertial Sensor Technology Trends," *Ieee Sensors Journal,* vol. 1, pp. 332-339, Dec 2001.

[50] K. Aminian and B. Najafi, "Capturing human motion using body-fixed sensors: outdoor measurement and clinical applications," *Computer Animation and Virtual Worlds,* vol. 15, pp. 79-94, May 2004.

[51] M. J. Mathie, A. C. F. Coster, N. H. Lovell, and B. G. Celler, "Accelerometry: providing an integrated, practical method for long-term, ambulatory monitoring of human movement," *Physiological Measurement*, vol. 25, pp. R1-R20, Apr 2004.

[52] W. Zijlstra and A. L. Hof, "Assessment of spatio-temporal gait parameters from trunk accelerations during human walking," *Gait & Posture*, vol. 18, pp. 1-10, Oct 2003.

[53] F. Paoletti, M. A. Gretillat, and N. F. deRooij, "A silicon micromachined vibrating gyroscope with piezoresistive detection and electromagnetic excitation," *Ninth Annual International Workshop on Micro Electro Mechanical Systems, Ieee Proceedings*, pp. 162-167, 1996.

[54] K. Y. Tong and M. H. Granat, "A practical gait analysis system using gyroscopes," *Medical Engineering & Physics*, vol. 21, pp. 87-94, Mar 1999.

[55] D. Roetenberg, H. J. Luinge, C. T. Baten, and P. H. Veltink, "Compensation of magnetic disturbances improves inertial and magnetic sensing of human body segment orientation," *IEEE Trans Neural Syst Rehabil Eng*, vol. 13, pp. 395-405, Sep 2005.

[56] S. Bonnet and R. Heliot, "A magnetometer-based approach for studying human movements," *IEEE Trans Biomed Eng*, vol. 54, pp. 1353-5, Jul 2007.

[57] N. Ahmad, R. A. R. Ghazilla, N. M. Khairi, and V. Kasi, "Reviews on Various Inertial Measurement Unit (IMU) Sensor Applications."

[58] R. Zhu and Z. Y. Zhou, "A real-time articulated human motion tracking using tri-axis inertial/magnetic sensors package," *Ieee Transactions on Neural Systems and Rehabilitation Engineering*, vol. 12, pp. 295-302, Jun 2004.

[59] M. J. Mathie, B. G. Celler, N. H. Lovell, and A. C. F. Coster, "Classification of basic daily movements using a triaxial accelerometer," *Medical & Biological Engineering & Computing*, vol. 42, pp. 679-687, Sep 2004.

[60] B. Najafi, K. Aminian, A. Paraschiv-Ionescu, F. Loew, C. J. Bula, and P. Robert, "Ambulatory system for human motion analysis using a kinematic sensor: Monitoring of daily physical activity in the elderly," *Ieee Transactions on Biomedical Engineering*, vol. 50, pp. 711-723, Jun 2003.

[61] M. P. Lawton and E. M. Brody, "Assessment of older people: self-maintaining and instrumental activities of daily living," *Gerontologist*, vol. 9, pp. 179-86, Autumn 1969.

[62] P. N. Ainslie, T. Reilly, and K. R. Westerterp, "Estimating human energy expenditure - A review of techniques with particular reference to doubly labelled water," *Sports Medicine*, vol. 33, pp. 683-698, 2003.

[63] K. Y. Chen and D. R. Bassett, "The technology of accelerometry-based activity monitors: Current and future," *Medicine and Science in Sports and Exercise*, vol. 37, pp. S490-S500, Nov 2005.

[64] C. V. Bouten, K. R. Westerterp, M. Verduin, and J. D. Janssen, "Assessment of Energy-Expenditure for Physical-Activity Using a Triaxial Accelerometer," *Medicine and Science in Sports and Exercise*, vol. 26, pp. 1516-1523, Dec 1994.

[65] T. C. Wong, J. G. Webster, H. J. Montoye, and R. Washburn, "Portable

Accelerometer Device for Measuring Human Energy-Expenditure," *Ieee Transactions on Biomedical Engineering,* vol. 28, pp. 467-471, 1981.

[66] H. J. Montoye, R. Washburn, S. Servais, A. Ertl, J. G. Webster, and F. J. Nagle, "Estimation of Energy-Expenditure by a Portable Accelerometer," *Medicine and Science in Sports and Exercise,* vol. 15, pp. 403-407, 1983.

[67] P. S. Freedson, E. Melanson, and J. Sirard, "Calibration of the Computer Science and Applications, Inc. accelerometer," *Medicine and Science in Sports and Exercise,* vol. 30, pp. 777-781, May 1998.

[68] D. Hendelman, K. Miller, C. Baggett, E. Debold, and P. Freedson, "Validity of accelerometry for the assessment of moderate intensity physical activity in the field," *Medicine and science in sports and exercise,* vol. 32, pp. S442-9, 09/ 2000.

[69] N. Y. J. M. Leenders, T. E. Nelson, and W. M. Sherman, "Ability of different physical activity monitors to detect movement during treadmill walking," *International Journal of Sports Medicine,* vol. 24, pp. 43-50, Jan 2003.

[70] A. G. Brooks, S. M. Gunn, R. T. Withers, C. J. Gore, and J. L. Plummer, "Predicting walking METs and energy expenditure from speed or accelerometry," *Med Sci Sports Exerc,* vol. 37, pp. 1216-23, Jul 2005.

[71] A. M. Swartz, S. J. Strath, D. R. Bassett, W. L. O'Brien, G. A. King, and B. E. Ainsworth, "Estimation of energy expenditure using CSA accelerometers at hip and wrist sites," *Medicine and Science in Sports and Exercise,* vol. 32, pp. S450-S456, Sep 2000.

[72] D. P. Heil, "Predicting activity energy expenditure using the Actical (R) activity monitor," *Research Quarterly for Exercise and Sport,* vol. 77, pp. 64-80, Mar 2006.

[73] S. E. Crouter, K. G. Clowers, and D. R. Bassett, "A novel method for using accelerometer data to predict energy expenditure," *Journal of Applied Physiology,* vol. 100, pp. 1324-1331, Apr 2006.

[74] S. E. Crouter and D. R. Bassett, "A new 2-regression model for the Actical accelerometer," *British Journal of Sports Medicine,* vol. 42, pp. 217-224, Mar 2008.

[75] S. E. Crouter, E. Kuffel, J. D. Haas, E. A. Frongillo, and D. R. Bassett, Jr., "Refined two-regression model for the ActiGraph accelerometer," *Med Sci Sports Exerc,* vol. 42, pp. 1029-37, May 2010.

[76] A. G. Bonomi, G. Plasqui, A. H. Goris, and K. R. Westerterp, "Improving assessment of daily energy expenditure by identifying types of physical activity with a single accelerometer," *J Appl Physiol (1985),* vol. 107, pp. 655-61, Sep 2009.

[77] J. Lester, T. Choudhury, N. Kern, G. Borriello, and B. Hannaford, "A Hybrid Discriminative/Generative Approach for Modeling Human Activities," *19th International Joint Conference on Artificial Intelligence (Ijcai-05),* pp. 766-772, 2005.

[78] J. Parkka, M. Ermes, P. Korpipaa, J. Mantyjarvi, J. Peltola, and I. Korhonen, "Activity classification using realistic data from wearable sensors," *Information*

Technology in Biomedicine, IEEE Transactions on, vol. 10, pp. 119-128, 2006.

[79] M. Ermes, J. Parkka, J. Mantyjarvi, and I. Korhonen, "Detection of daily activities and sports with wearable sensors in controlled and uncontrolled conditions," *Ieee Transactions on Information Technology in Biomedicine,* vol. 12, pp. 20-26, Jan 2008.

[80] L. Bao and S. S. Intille, "Activity recognition from user-annotated acceleration data," *Pervasive Computing, Proceedings,* vol. 3001, pp. 1-17, 2004.

[81] F. Foerster, M. Smeja, and J. Fahrenberg, "Detection of posture and motion by accelerometry: a validation study in ambulatory monitoring," *Computers in Human Behavior,* vol. 15, pp. 571-583, Sep 1999.

[82] D. M. Pober, J. Staudenmayer, C. Raphael, and P. S. Freedson, "Development of novel techniques to classify physical activity mode using accelerometers," *Medicine and Science in Sports and Exercise,* vol. 38, pp. 1626-1634, Sep 2006.

[83] M. J. Mathie, B. G. Celler, N. H. Lovell, and A. C. F. Coster, "Classification of basic daily movements using a triaxial accelerometer," *Medical and Biological Engineering and Computing,* vol. 42, pp. 679-687, 2004/09/01 2004.

[84] D. M. Karantonis, M. R. Narayanan, M. Mathie, N. H. Lovell, and B. G. Celler, "Implementation of a real-time human movement classifier using a triaxial accelerometer for ambulatory monitoring," *Information Technology in Biomedicine, IEEE Transactions on,* vol. 10, pp. 156-167, 2006.

[85] P. H. Veltink, H. J. Bussmann, W. De Vries, W. L. Martens, and R. C. Van Lummel, "Detection of static and dynamic activities using uniaxial accelerometers," *Rehabilitation Engineering, IEEE Transactions on,* vol. 4, pp. 375-385, 1996.

[86] N. Ravi, N. Dandekar, P. Mysore, and M. L. Littman, "Activity recognition from accelerometer data," presented at the Proceedings of the 17th conference on Innovative applications of artificial intelligence - Volume 3, Pittsburgh, Pennsylvania, 2005.

[87] L. Xi, Y. Bin, and R. M. Aarts, "Single-accelerometer-based daily physical activity classification," in *Engineering in Medicine and Biology Society, 2009. EMBC 2009. Annual International Conference of the IEEE,* 2009, pp. 6107-6110.

[88] M. H. Lee, J. Kim, K. Kim, I. Lee, S. H. Jee, and S. K. Yoo, "Physical Activity Recognition Using a Single Tri-Axis Accelerometer," *Wcecs 2009: World Congress on Engineering and Computer Science, Vols I and Ii,* pp. 14-17, 2009.

[89] A. G. Bonomi, A. H. C. Goris, B. Yin, and K. R. Westerterp, "Detection of Type, Duration, and Intensity of Physical Activity Using an Accelerometer," *Medicine and Science in Sports and Exercise,* vol. 41, pp. 1770-1777, Sep 2009.

[90] A. M. Khan, Y. K. Lee, S. Y. Lee, and T. S. Kim, "A Triaxial Accelerometer-Based Physical-Activity Recognition via Augmented-Signal Features and a Hierarchical Recognizer," *Ieee Transactions on Information Technology in Biomedicine,* vol. 14, pp. 1166-1172, Sep 2010.

[91] S. J. Preece, J. Y. Goulermas, L. P. Kenney, D. Howard, K. Meijer, and R. Crompton, "Activity identification using body-mounted sensors--a review of

classification techniques," *Physiol Meas,* vol. 30, pp. R1-33, Apr 2009.
[92] S. Dua, U. R. Acharya, and P. Dua, *Machine Learning in Healthcare Informatics*: Springer, 2013.
[93] P. Chowriappa, S. Dua, and Y. Todorov, "Introduction to Machine Learning in Healthcare Informatics," in *Machine Learning in Healthcare Informatics*, ed: Springer, 2014, pp. 1-23.
[94] H. Zhang, D. D. Yao, and N. Ramakrishnan, "POSTER: A semantic-aware approach to reasoning about network traffic relations," presented at the Proceedings of the 2013 ACM SIGSAC conference on Computer & communications security, Berlin, Germany, 2013.
[95] H. Zhang, D. D. Yao, and N. Ramakrishnan, "Detection of Stealthy Malware Activities with Traffic Causality and Scalable Triggering Relation Discovery," 2014.
[96] D. Jurafsky and J. H. Martin, *Speech and Language Processing: An Introduction to Natural Language Processing, Computational Linguistics, and Speech Recognition*: Pearson Prentice Hall, 2009.
[97] A. K. Jain, R. P. W. Duin, and J. C. Mao, "Statistical pattern recognition: A review," *Ieee Transactions on Pattern Analysis and Machine Intelligence,* vol. 22, pp. 4-37, Jan 2000.
[98] R. O. Duda, P. E. Hart, and D. G. Stork, *Pattern classification*: Wiley, 2001.
[99] S. Theodoridis and K. Koutroumbas, *Pattern Recognition*: Elsevier Science, 2006.
[100] A. R. Webb and K. D. Copsey, *Statistical Pattern Recognition*: Wiley, 2011.
[101] N. Cristianini and J. Shawe-Taylor, *An Introduction to Support Vector Machines and Other Kernel-based Learning Methods*: Cambridge University Press, 2000.
[102] V. N. Vapnik, *Statistical learning theory*: Wiley, 1998.
[103] V. Vapnik, S. E. Golowich, and A. Smola, "Support vector method for function approximation, regression estimation, and signal processing," *Advances in Neural Information Processing Systems 9,* vol. 9, pp. 281-287, 1997.
[104] N. Nuryani, S. S. H. Ling, and H. T. Nguyen, "Electrocardiographic Signals and Swarm-Based Support Vector Machine for Hypoglycemia Detection," *Annals of Biomedical Engineering,* vol. 40, pp. 934-945, Apr 2012.
[105] J. Weston, S. Mukherjee, O. Chapelle, M. Pontil, T. Poggio, and V. Vapnik, "Feature selection for SVMs," *Advances in Neural Information Processing Systems 13*, vol. 13, pp. 668-674, 2001.
[106] A. Widodo and B. S. Yang, "Support vector machine in machine condition monitoring and fault diagnosis," *Mechanical Systems and Signal Processing,* vol. 21, pp. 2560-2574, Aug 2007.
[107] V. Cherkassky, "The nature of statistical learning theory~," *IEEE Trans Neural Netw,* vol. 8, p. 1564, 1997.
[108] F. Cucker and S. Smale, "On the mathematical foundations of learning," *Bulletin of the American Mathematical Society,* vol. 39, pp. 1-49, 2002.
[109] C. M. Bishop, *Neural Networks for Pattern Recognition*: Clarendon Press, 1995.
[110] C. J. C. Burges and B. Scholkopf, "Improving the accuracy and speed of support

vector machines," *Advances in Neural Information Processing Systems 9,* vol. 9, pp. 375-381, 1997.

[111] C. Gold, A. Holub, and P. Sollich, "Bayesian approach to feature selection and parameter tuning for support vector machine classifiers," *Neural Networks,* vol. 18, pp. 693-701, Jun-Jul 2005.

[112] S. S. Keerthi, "Efficient tuning of SVM hyperparameters using radius/margin bound and iterative algorithms," *Ieee Transactions on Neural Networks,* vol. 13, pp. 1225-1229, Sep 2002.

[113] J. Li and S. K. Halgamuge, "Improving training speed of Support Vector Machines by creating exploitable trends of Lagrangian variables: an application to DNA splice site detection," *Proceedings of the Frontiers in the Convergence of Bioscience and Information Technologies*, pp. 230-233, 2007.

[114] J. A. K. Suykens and J. Vandewalle, "Least Squares Support Vector Machine Classifiers," *Neural Processing Letters,* vol. 9, pp. 293-300, 1999/06/01 1999.

[115] B. Najafi, K. Aminian, F. Loew, Y. Blanc, and P. A. Robert, "Measurement of stand-sit and sit-stand transitions using a miniature gyroscope and its application in fall risk evaluation in the elderly," *Ieee Transactions on Biomedical Engineering,* vol. 49, pp. 843-851, Aug 2002.

[116] B. Coley, B. Najafi, A. Paraschiv-Ionescu, and K. Aminian, "Stair climbing detection during daily physical activity using a miniature gyroscope," *Gait Posture,* vol. 22, pp. 287-294, Dec 2005.

[117] M. J. Mathie, A. C. F. Coster, N. H. Lovell, and B. G. Celler, "Detection of daily physical activities using a triaxial accelerometer," *Med Biol Eng Comput,* vol. 41, pp. 296-301, May 2003.

[118] J. Fahrenberg, W. Muller, F. Foerster, and M. Smeja, "A multi-channel investigation of physical activity," *Journal of Psychophysiology,* vol. 10, pp. 209-217, 1996.

[119] J. Fahrenberg, F. Foerster, M. Smeja, and W. Muller, "Assessment of posture and motion by multichannel piezoresistive accelerometer recordings," *Psychophysiology,* vol. 34, pp. 607-612, Sep 1997.

[120] S. H. Lee, H. D. Park, S. Y. Hong, K. J. Lee, and Y. H. Kim, "A study on the activity classification using a triaxial accelerometer," in *Engineering in Medicine and Biology Society, 2003. Proceedings of the 25th Annual International Conference of the IEEE,* 2003, pp. 2941-2943 Vol.3.

[121] J. Parkka, M. Ermes, P. Korpipaa, J. Mantyjarvi, J. Peltola, and I. Korhonen, "Activity classification using realistic data from wearable sensors," *Ieee Transactions on Information Technology in Biomedicine,* vol. 10, pp. 119-128, Jan 2006.

[122] U. Maurer, A. Rowe, A. Smailagic, and D. Siewiorek, "Location and activity recognition using eWatch: A wearable sensor platform," *Ambient Intelligence in Everday Life,* vol. 3864, pp. 86-102, 2006.

[123] F. Foerster and J. Fahrenberg, "Motion pattern and posture: Correctly assessed by calibrated accelerometers," *Behavior Research Methods Instruments & Computers,* vol. 32, pp. 450-457, Aug 2000.

[124] J. B. J. Bussmann, W. L. J. Martens, J. H. M. Tulen, F. C. Schasfoort, H. J. G. van den Berg-Emons, and H. J. Stam, "Measuring daily behavior using ambulatory accelerometry: The activity monitor," *Behavior Research Methods Instruments & Computers*, vol. 33, pp. 349-356, Aug 2001.

[125] K. Zhang, M. Sun, D. K. Lester, F. X. Pi-Sunyer, C. N. Boozer, and R. W. Longman, "Assessment of human locomotion by using an insole measurement system and artificial neural networks," *Journal of Biomechanics*, vol. 38, pp. 2276-2287, Nov 2005.

[126] M. N. Nyan, F. E. Tay, K. H. Seah, and Y. Y. Sitoh, "Classification of gait patterns in the time-frequency domain," *Journal of Biomechanics*, vol. 39, pp. 2647-56, 2006.

[127] J. Baek, G. Lee, W. Park, and B. J. Yun, "Accelerometer signal processing for user activity detection," *Knowledge-Based Intelligent Information and Engineering Systems, Pt 3, Proceedings*, vol. 3215, pp. 610-617, 2004.

[128] S. Pirttikangas, K. Fujinami, and T. Nakajima, "Feature selection and activity recognition from wearable sensors," *Ubiquitous Computing Systems, Proceedings*, vol. 4239, pp. 516-527, 2006.

[129] T. Huynh and B. Schiele, "Towards Less Supervision in Activity Recognition from Wearable Sensors," in *Wearable Computers, 2006 10th IEEE International Symposium on*, 2006, pp. 3-10.

[130] A. Krause, M. Ihmig, E. Rankin, D. Leong, G. Smriti, D. Siewiorek, *et al.*, "Trading off prediction accuracy and power consumption for context-aware wearable computing," in *Wearable Computers, 2005. Proceedings. Ninth IEEE International Symposium on*, 2005, pp. 20-26.

[131] M. Lee, M. Roan, B. Smith, and T. E. Lockhart, "Gait analysis to classify external load conditions using linear discriminant analysis," *Human Movement Science*, vol. 28, pp. 226-235, Apr 2009.

[132] F. R. Allen, E. Ambikairajah, N. H. Lovell, and B. G. Celler, "Classification of a known sequence of motions and postures from accelerometry data using adapted Gaussian mixture models," *Physiological Measurement*, vol. 27, pp. 935-951, Oct 2006.

[133] J. Lester, T. Choudhury, and G. Borriello, "A practical approach to recognizing physical activities," *Pervasive Computing, Proceedings*, vol. 3968, pp. 1-16, 2006.

[134] S.-W. Lee and K. Mase, "Activity and location recognition using wearable sensors," *Pervasive Computing, IEEE*, vol. 1, pp. 24-32, 2002.

[135] K. Van Laerhoven and O. Cakmakci, "What shall we teach our pants?," in *Wearable Computers, The Fourth International Symposium on*, 2000, pp. 77-83.

[136] A. Krause, D. P. Siewiorek, A. Smailagic, and J. Farringdon, "Unsupervised, dynamic identification of physiological and activity context in wearable computing," in *Wearable Computers, 2003. Proceedings. Seventh IEEE International Symposium on*, 2003, pp. 88-97.

[137] A. T. M. Willemsen, F. Bloemhof, and H. B. K. Boom, "Automatic Stance-Swing Phase Detection from Accelerometer Data for Peroneal Nerve-

Stimulation," *Ieee Transactions on Biomedical Engineering,* vol. 37, pp. 1201-1208, Dec 1990.

[138] K. Aminian, K. Rezakhanlou, E. De Andres, C. Fritsch, P. F. Leyvraz, and P. Robert, "Temporal feature estimation during walking using miniature accelerometers: an analysis of gait improvement after hip arthroplasty," *Medical & Biological Engineering & Computing,* vol. 37, pp. 686-691, Nov 1999.

[139] R. E. Mayagoitia, A. V. Nene, and P. H. Veltink, "Accelerometer and rate gyroscope measurement of kinematics: an inexpensive alternative to optical motion analysis systems," *Journal of Biomechanics,* vol. 35, pp. 537-542, Apr 2002.

[140] C. A. E. Dyer, C. L. Watkins, C. Gould, and J. Rowe, "Risk-factor assessment for falls: from a written checklist to the penless clinic," *Age and Ageing,* vol. 27, pp. 569-572, Sep 1998.

[141] H.-C. Huang, "A checklist for assessing the risk of falls among the elderly," *Journal of Nursing Research,* vol. 12, pp. 131-142, 2004.

[142] S. R. Lord, C. Sherrington, H. B. Menz, and J. C. T. Close, *Falls in Older People: Risk Factors and Strategies for Prevention*: Cambridge University Press, 2007.

[143] M. Piirtola and P. Era, "Force platform measurements as predictors of falls among older people - A review," *Gerontology,* vol. 52, pp. 1-16, 2006.

[144] D. J. Hewson, N. K. Singh, H. Snoussi, and J. Duchene, "Classification of elderly as fallers and non-fallers using centre of pressure velocity," *2010 Annual International Conference of the Ieee Engineering in Medicine and Biology Society (Embc),* pp. 3678-3681, 2010.

[145] K. E. Bigelow and N. Berme, "Development of a Protocol for Improving the Clinical Utility of Posturography as a Fall-Risk Screening Tool," *Journals of Gerontology Series a-Biological Sciences and Medical Sciences,* vol. 66, pp. 228-233, Feb 2011.

[146] L. K. Boulgarides, S. M. McGinty, J. A. Willett, and C. W. Barnes, "Use of clinical and, impairment-based tests to predict falls by community-dwelling older adults," *Physical Therapy,* vol. 83, pp. 328-339, Apr 2003.

[147] B. E. Maki, P. J. Holliday, and A. K. Topper, "A Prospective-Study of Postural Balance and Risk of Falling in an Ambulatory and Independent Elderly Population," *Journals of Gerontology,* vol. 49, pp. M72-M84, Mar 1994.

[148] V. S. Stel, J. H. Smit, S. M. F. Pluijm, and P. Lips, "Balance and mobility performance as treatable risk factors for recurrent falling in older persons," *Journal of Clinical Epidemiology,* vol. 56, pp. 659-668, Jul 2003.

[149] P. B. Thapa, P. Gideon, K. G. Brockman, R. L. Fought, and W. A. Ray, "Clinical and biomechanical measures of balance as fall predictors in ambulatory nursing home residents," *Journals of Gerontology Series a-Biological Sciences and Medical Sciences,* vol. 51, pp. M239-M246, Sep 1996.

[150] A. Bergland and T. B. Wyller, "Risk factors for serious fall related injury in elderly women living at home," *Injury Prevention,* vol. 10, pp. 308-313, Oct 2004.

[151] J. Swanenburg, E. D. de Bruin, D. Uebelhart, and T. Mulder, "Falls prediction

in elderly people: A 1-year prospective study," *Gait & Posture,* vol. 31, pp. 317-321, Mar 2010.

[152] B. M. Shin, S. J. Han, J. H. Jung, J. E. Kim, and F. Fregni, "Effect of mild cognitive impairment on balance," *Journal of the Neurological Sciences,* vol. 305, pp. 121-125, Jun 15 2011.

[153] K. L. Johansen, G. M. Chertow, A. V. Ng, K. Mulligan, S. Carey, P. Y. Schoenfeld, *et al.*, "Physical activity levels in patients on hemodialysis and healthy sedentary controls," *Kidney International,* vol. 57, pp. 2564-2570, Jun 2000.

[154] B. Najafi, K. Aminian, F. Loew, Y. Blanc, and P. Robert, "Falling risk evaluation in elderly using miniature gyroscope," *1st Annual International Ieee-Embs Special Topic Conference on Microtechnologies in Medicine & Biology, Proceedings*, pp. 557-561, 2000.

[155] D. Giansanti, "Investigation of fall-risk using a wearable device with accelerometers and rate gyroscopes," *Physiological Measurement,* vol. 27, pp. 1081-1090, Nov 2006.

[156] D. Giansanti, G. Maccioni, S. Cesinaro, F. Benvenuti, and V. Macellari, "Assessment of fall-risk by means of a neural network based on parameters assessed by a wearable device during posturography," *Medical Engineering & Physics,* vol. 30, pp. 367-372, Apr 2008.

[157] M. O'Sullivan, C. Blake, C. Cunningham, G. Boyle, and C. Finucane, "Correlation of accelerometry with clinical balance tests in older fallers and non-fallers," *Age and Ageing,* vol. 38, pp. 308-313, May 2009.

[158] M. R. Narayanan, S. J. Redmond, M. E. Scalzi, S. R. Lord, B. G. Celler, and N. H. Lovell, "Longitudinal Falls-Risk Estimation Using Triaxial Accelerometry," *Ieee Transactions on Biomedical Engineering,* vol. 57, pp. 534-541, Mar 2010.

[159] L. Ying, S. J. Redmond, W. Ning, F. Blumenkron, M. R. Narayanan, and N. H. Lovell, "Spectral Analysis of Accelerometry Signals From a Directed-Routine for Falls-Risk Estimation," *Biomedical Engineering, IEEE Transactions on,* vol. 58, pp. 2308-2315, 2011.

[160] M. Gietzelt, G. Nemitz, K. H. Wolf, H. M. Z. Schwabedissen, R. Haux, and M. Marschollek, "A clinical study to assess fall risk using a single waist accelerometer," *Informatics for Health & Social Care,* vol. 34, pp. 181-188, 2009.

[161] M. Marschollek, G. Nemitz, M. Gietzelt, K. H. Wolf, H. M. Z. Schwabedissen, and R. Haux, "Predicting in-patient falls in a geriatric clinic A clinical study combining assessment data and simple sensory gait measurements," *Zeitschrift Fur Gerontologie Und Geriatrie,* vol. 42, pp. 317-321, Aug 2009.

[162] B. R. Greene, A. O'Donovan, R. Romero-Ortuno, L. Cogan, C. N. Scanaill, and R. A. Kenny, "Quantitative Falls Risk Assessment Using the Timed Up and Go Test," *Ieee Transactions on Biomedical Engineering,* vol. 57, pp. 2918-2926, Dec 2010.

[163] M. Marschollek, A. Rehwald, K. H. Wolf, M. Gietzelt, G. Nemitz, H. M. zu Schwabedissen, *et al.*, "Sensors vs. experts - a performance comparison of

sensor-based fall risk assessment vs. conventional assessment in a sample of geriatric patients," *BMC Med Inform Decis Mak,* vol. 11, p. 48, 2011.

[164] A. Weiss, T. Herman, M. Plotnik, M. Brozgol, N. Giladi, and J. M. Hausdorff, "An instrumented timed up and go: the added value of an accelerometer for identifying fall risk in idiopathic fallers," *Physiological Measurement,* vol. 32, pp. 2003-2018, Dec 2011.

[165] I. Bautmans, B. Jansen, B. Van Keymolen, and T. Mets, "Reliability and clinical correlates of 3D-accelerometry based gait analysis outcomes according to age and fall-risk," *Gait & Posture,* vol. 33, pp. 366-372, Mar 2011.

[166] B. Caby, S. Kieffer, M. de Saint Hubert, G. Cremer, and B. Macq, "Feature extraction and selection for objective gait analysis and fall risk assessment by accelerometry," *Biomedical Engineering Online,* vol. 10, Jan 9 2011.

[167] A. T. Barth, M. A. Hanson, H. C. Powell, and J. Lach, "TEMPO 3.1: A Body Area Sensor Network Platform for Continuous Movement Assessment," *Sixth International Workshop on Wearable and Implantable Body Sensor Networks, Proceedings,* pp. 71-76, 2009.

[168] C. V. C. Bouten, K. T. M. Koekkoek, M. Verduin, R. Kodde, and J. D. Janssen, "A triaxial accelerometer and portable data processing unit for the assessment of daily physical activity," *Ieee Transactions on Biomedical Engineering,* vol. 44, pp. 136-147, Mar 1997.

[169] C. C. Chang and C. J. Lin, "LIBSVM: A Library for Support Vector Machines," *Acm Transactions on Intelligent Systems and Technology,* vol. 2, 2011.

[170] R. Soangra and T. E. Lockhart, "A comparative study for performance evaluation of sit-to-stand task with body worn sensor and existing laboratory methods," *Biomed Sci Instrum,* vol. 48, pp. 407-14, 2012.

[171] H. J. Luinge, *Inertial sensing of human movement*: Twente University Press, 2002.

[172] N. E. Huang, Z. Shen, S. R. Long, M. L. C. Wu, H. H. Shih, Q. N. Zheng*, et al.*, "The empirical mode decomposition and the Hilbert spectrum for nonlinear and non-stationary time series analysis," *Proceedings of the Royal Society of London Series a-Mathematical Physical and Engineering Sciences,* vol. 454, pp. 903-995, Mar 8 1998.

[173] N. E. Huang, Z. Shen, and S. R. Long, "A new view of nonlinear water waves: The Hilbert spectrum," *Annual Review of Fluid Mechanics,* vol. 31, pp. 417-457, 1999.

[174] Z. Wu and N. E. Huang, "ENSEMBLE EMPIRICAL MODE DECOMPOSITION: A NOISE-ASSISTED DATA ANALYSIS METHOD," *Advances in Adaptive Data Analysis,* vol. 01, pp. 1-41, 2009/01/01 2009.

[175] J. A. Zhang, R. Q. Yan, R. X. Gao, and Z. H. Feng, "Performance enhancement of ensemble empirical mode decomposition," *Mechanical Systems and Signal Processing,* vol. 24, pp. 2104-2123, Oct 2010.

[176] J. Zhang, R. Yan, R. X. Gao, and Z. Feng, "Performance enhancement of ensemble empirical mode decomposition," *Mechanical Systems and Signal Processing,* vol. 24, pp. 2104-2123, 2010.

[177] M. Whittle, *Gait Analysis: An Introduction*: Butterworth-Heinemann, 2002.
[178] S. Cuccurullo, *Physical Medicine and Rehabilitation Board Review*: Demos, 2004.
[179] D. Podsiadlo and S. Richardson, "The Timed up and Go - a Test of Basic Functional Mobility for Frail Elderly Persons," *Journal of the American Geriatrics Society,* vol. 39, pp. 142-148, Feb 1991.
[180] S. L. Whitney, D. M. Wrisley, G. F. Marchetti, M. A. Gee, M. S. Redfern, and J. M. Furman, "Clinical measurement of sit-to-stand performance in people with balance disorders: Validity of data for the five-times-sit-to-stand test," *Physical Therapy,* vol. 85, pp. 1034-1045, Oct 2005.
[181] B. Etnyre and D. Q. Thomas, "Event standardization of sit-to-stand movements," *Physical Therapy,* vol. 87, pp. 1651-1666, Dec 2007.
[182] T. A. Buckley, C. Pitsikoulis, and C. J. Hass, "Dynamic postural stability during sit-to-walk transitions in Parkinson disease patients," *Movement Disorders,* vol. 23, pp. 1274-1280, Jul 15 2008.
[183] A. Kerr, D. Rafferty, K. M. Kerr, and B. Durward, "Timing phases of the sit-to-walk movement: Validity of a clinical test," *Gait & Posture,* vol. 26, pp. 11-16, Jun 2007.
[184] T. Buckley, C. Pitsikoulis, E. Barthelemy, and C. J. Hass, "Age impairs sit-to-walk motor performance," *Journal of Biomechanics,* vol. 42, pp. 2318-2322, Oct 16 2009.
[185] A. Kerr, B. Durward, and K. M. Kerr, "Defining phases for the sit-to-walk movement," *Clinical Biomechanics,* vol. 19, pp. 385-390, May 2004.
[186] X. Wu and T. E. Lockhart, "Fall risks assessment for the community dwelling obese elderly using wearable sensors," in *American Soceity of Biomechanics*, University of Nebraska at Omaha, Nebraska. USA., 2013.
[187] C. Toulotte, A. Thevenon, E. Watelain, and C. Fabre, "Identification of healthy elderly fallers and non-fallers by gait analysis under dual-task conditions," *Clinical Rehabilitation,* vol. 20, pp. 269-276, Mar 2006.
[188] G. M. Gehlsen and M. H. Whaley, "Falls in the elderly: Part I, Gait," *Arch Phys Med Rehabil,* vol. 71, pp. 735-8, Sep 1990.
[189] M. Pijnappels, M. F. Bobbert, and J. H. van Dieen, "Push-off reactions in recovery after tripping discriminate young subjects, older non-falters and older fallers," *Gait & Posture*, vol. 21, pp. 388-394, Jun 2005.
[190] B. E. Maki, "Gait changes in older adults: Predictors of falls or indicators of fear?," *Journal of the American Geriatrics Society,* vol. 45, pp. 313-320, Mar 1997.
[191] C. Y. Cho and G. Kamen, "Detecting balance deficits in frequent fallers using clinical and quantitative evaluation tools," *Journal of the American Geriatrics Society,* vol. 46, pp. 426-430, Apr 1998.
[192] J. L. Medell and N. B. Alexander, "A clinical measure of maximal and rapid stepping in older women," *Journals of Gerontology Series a-Biological Sciences and Medical Sciences,* vol. 55, pp. M429-M433, Aug 2000.
[193] F. J. Imms and O. G. Edholm, "Studies of gait and mobility in the elderly," *Age*

Ageing, vol. 10, pp. 147-56, Aug 1981.
[194] L. Wolfson, R. Whipple, P. Amerman, and J. N. Tobin, "Gait assessment in the elderly: a gait abnormality rating scale and its relation to falls," *J Gerontol,* vol. 45, pp. M12-9, Jan 1990.
[195] E. P. Doheny, C. W. Fan, T. Foran, B. R. Greene, C. Cunningham, and R. A. Kenny, "An instrumented sit-to-stand test used to examine differences between older fallers and non-fallers," *2011 Annual International Conference of the Ieee Engineering in Medicine and Biology Society (Embc),* pp. 3063-3066, 2011.
[196] S. Buatois, D. Miljkovic, P. Manckoundia, R. Gueguen, P. Miget, G. Vancon*, et al.*, "Five times sit to stand test is a predictor of recurrent falls in healthy community-living subjects aged 65 and older," *Journal of the American Geriatrics Society,* vol. 56, pp. 1575-1577, Aug 2008.
[197] G. Kamen, C. Patten, C. D. Du, and S. Sison, "An accelerometry-based system for the assessment of balance and postural sway," *Gerontology,* vol. 44, pp. 40-45, Jan-Feb 1998.
[198] L. Wolf, H. Jhuang, and T. Hazan, "Modeling appearances with low-rank SVM," *2007 Ieee Conference on Computer Vision and Pattern Recognition, Vols 1-8,* pp. 990-995, 2007.
[199] H. S. Hota, A. K. Shrivas, and S. K. Singhai, "Artificial Neural Network, Decision Tree and Statistical Techniques Applied for Designing and Developing E-mail Classifier," *Training,* vol. 40, p. 60.
[200] I. T. Jolliffe, *Principal Component Analysis*: Springer, 2002.
[201] A. N. Gorban, *Principal Manifolds for Data Visualization and Dimension Reduction*: Springer, 2007.
[202] B. Hudgins, P. Parker, and R. N. Scott, "A new strategy for multifunction myoelectric control," *IEEE Trans Biomed Eng,* vol. 40, pp. 82-94, Jan 1993.
[203] A. Hreljac and P. E. Martin, "The Relationship between Smoothness and Economy during Walking," *Biological Cybernetics,* vol. 69, pp. 213-218, Jul 1993.
[204] A. N. Gorban, B. Kgl, D. C. Wunsch, and A. Zinovyev, *Principal Manifolds for Data Visualization and Dimension Reduction*: Springer Publishing Company, Incorporated, 2007.
[205] J. G. Barton and A. Lees, "An application of neural networks for distinguishing gait patterns on the basis of hip-knee joint angle diagrams," *Gait & Posture*, vol. 5, pp. 28-33, 1997.
[206] R. Begg and J. Kamruzzaman, "A machine learning approach for automated recognition of movement patterns using basic, kinetic and kinematic gait data," *J Biomech,* vol. 38, pp. 401-8, Mar 2005.
[207] G. A. Cavagna, "Force platforms as ergometers," *J Appl Physiol,* vol. 39, pp. 174-9, Jul 1975.
[208] G. A. Cavagna, N. C. Heglund, and C. R. Taylor, "Mechanical work in terrestrial locomotion: two basic mechanisms for minimizing energy expenditure," *Am J Physiol,* vol. 233, pp. R243-61, Nov 1977.
[209] G. A. Cavagna, F. P. Saibene, and R. Margaria, "External work in walking," *J*

Appl Physiol, vol. 18, pp. 1-9, Jan 1963.
[210] C. R. Lee and C. T. Farley, "Determinants of the center of mass trajectory in human walking and running," *J Exp Biol,* vol. 201, pp. 2935-44, Nov 1998.
[211] V. T. Inman, "Human locomotion," *Can Med Assoc J,* vol. 94, pp. 1047-54, May 14 1966.
[212] J. B. Saunders, V. T. Inman, and H. D. Eberhart, "The major determinants in normal and pathological gait," *J Bone Joint Surg Am,* vol. 35-A, pp. 543-58, Jul 1953.
[213] E. Kellis and C. Liassou, "The effect of selective muscle fatigue on sagittal lower limb kinematics and muscle activity during level running," *J Orthop Sports Phys Ther,* vol. 39, pp. 210-20, Mar 2009.
[214] L. Lee and W. E. L. Grimson, "Gait analysis for recognition and classification," in *Automatic Face and Gesture Recognition, 2002. Proceedings. Fifth IEEE International Conference on*, 2002, pp. 148-155.
[215] P. Luukka and J. Lampinen, "Differential Evolution Classifier in Noisy Settings and with Interacting Variables," *Applied Soft Computing,* vol. 11, pp. 891-899, Jan 2011.
[216] D. F. Nettleton, A. Orriols-Puig, and A. Fornells, "A study of the effect of different types of noise on the precision of supervised learning techniques," *Artificial Intelligence Review,* vol. 33, pp. 275-306, Apr 2010.
[217] T. B. Trafalis and S. A. Alwazzi, "Support vector machine classification with noisy data: a second order cone programming approach," *International Journal of General Systems,* vol. 39, pp. 757-781, 2010.
[218] A. Christmann and I. Steinwart, "Consistency and robustness of kernel-based regression in convex risk minimization," *Bernoulli,* vol. 13, pp. 799-819, Aug 2007.